

Cite this: *J. Mater. Chem. C*, 2021,  
9, 16391

# Advances in applying C–H functionalization and naturally sourced building blocks in organic semiconductor synthesis

Liwen Xing<sup>a</sup> and Christine K. Luscombe<sup>†\*</sup>

Organic electronics is a rising field, with novel applications including but not limited to stretchable solar cells, flexible display screens, and biosensors. The high performance of these organic electronics is enabled by the outstanding optoelectronic and thermomechanical features of organic semiconducting materials. However, the production of the promising organic semiconducting materials at industrial scales has not yet become feasible, due to huge energy and capital costs in the large-scale synthesis as well as the potential damage to the environment and human health caused by vast hazardous chemical waste released. This review summarizes recent research advances in improving the environmental friendliness of the organic semiconducting material synthesis by applying atom economical C–H functionalization-based synthetic routes, minimizing hazardous chemical waste, lowering the energy consumption, and employing safe and abundant chemicals including naturally sourced semiconducting building blocks. This review showcases the remarkable progress that has been made towards the environmentally friendly organic semiconductor synthesis and provides insight for researchers developing green synthetic strategies and organic semiconductor building blocks in the future.

Received 1st September 2021,  
Accepted 20th October 2021

DOI: 10.1039/d1tc04128b

rsc.li/materials-c

## 1. Introduction

Organic semiconducting materials (OSMs) are promising materials for organic electronics in many applications, such as photovoltaics (OPVs),<sup>1,2</sup> light-emitting diodes (LEDs),<sup>3–5</sup> organic (OFETs),<sup>6–9</sup> and biomedical electronic devices.<sup>10,11</sup> They are intrinsically more flexible and stretchable compared to inorganic semiconducting materials such as silicon. In addition, their solution processibility makes them accessible to inexpensive and efficient manufacturing processes such as roll-to-roll printing, while their biocompatibility allows them to be applied as implantable medical devices in living organisms. The various chemical structures of the OSMs enable their wide range of electronic and optical tunability.

Despite these advantages of OSMs, there are some obstacles that hinder the large-scale manufacture and commercial viability of the OSMs. Besides the high material costs, one severe obstacle is the amplified negative environmental impacts associated with the conventional synthetic methods of OSMs in industrial scales, for example, large amounts of chemicals, energy, money, and time

wasted by lengthy synthetic routes, energy-intensive conditions employed, toxic and hazardous reagents used. Scheme 1 shows a few examples of OSMs and their conventional synthetic routes (Scheme 1).<sup>12–15</sup>

Thiophene and its derivatives are some of the most common building blocks in OSMs due to their excellent optical and electronic properties as well as their high thermal stability.<sup>16,17</sup> Poly(3-hexylthiophene) (P3HT) is a ubiquitous OSM that has been widely applied as an electron donor in OPV devices.<sup>18,19</sup> However, the current production process of thiophene is not environmentally friendly. It is synthesized *via* a vapor phase reaction that occurs at an exceedingly high temperature (~500 °C), which is highly energy-intensive and imposes safety issues.<sup>20</sup> Moreover, thiophene itself is toxic. Its release to the environment can cause long lasting harmful effects on to aquatic life.<sup>21–23</sup> Similarly, other common building blocks in OSMs, including furan, azoles, and other cyclic aromatic structures, also have certain levels of toxicity to living organisms and are prepared by harmful industrial processes,<sup>22–25</sup> which negatively impacts the environment.

The conventional synthetic methods for OSMs, which include Suzuki, Kumada, Negishi, and Stille couplings, are often multi-step processes which involve pre-functionalization of the starting materials (Scheme 1). The pre-functionalization steps include halogenation, boronation, stannylation, and other metalation reactions depending on the type of coupling. The long synthetic

<sup>a</sup> Molecular Engineering & Sciences Institute, University of Washington, Seattle, WA 98195, USA<sup>b</sup> Department of Material Science & Engineering, University of Washington, Seattle, WA 98195, USA<sup>†</sup> Current address: pi-Conjugated Polymers Unit, Okinawa Institute of Science and Technology Graduate University, Okinawa, 904-0495, Japan. E-mail: christine.luscombe@oist.jp



**Scheme 1** (a) Synthesis of diketopyrrolopyrrole (DPP) containing oligothiophenes via Suzuki coupling.<sup>12</sup> (b) Synthesis of P3HT via Kumada catalyst transfer polycondensation (KCTP).<sup>13</sup> (c) Synthesis of poly[4,4-bis(2-ethylhexyl)-4Hcyclopenta[2,1-b:3,4-b']dithiophene-2,6-diyl-alt-2,1,3-benzothiadiazole-4,7-diyl] (PCPDTBT) via Suzuki coupling.<sup>14</sup> (d) Synthesis of DPP containing copolymers (TDPP-BBT) via Stille coupling.<sup>15</sup>

process of OSMs results in waste of time and money and generation of a large amount of hazardous chemical waste and toxic byproducts, particularly the organotin byproducts generated from Stille coupling are virulent to humans.<sup>26–28</sup> Additionally, the use of scarce and toxic metal catalysts is environmentally unsustainable.

Many scientific endeavors have been made to improve the environmental impact of OSMs, including shortening the synthetic routes by adopting C–H functionalization, applying green solvents, replacing the toxic and scarce metal catalysts with earth abundant (first row) transition metal catalysts, reducing the energy consumption by performing the synthesis under ambient conditions, as well as utilizing naturally sourced building blocks.<sup>29–43</sup> This review highlights the progress on enhancing the environmental friendliness of synthetic protocols, consisting of

synthetic routes, reagents, reaction conditions, and building blocks of OSMs, made in the past four years to facilitate the large-scale production and commercialization of OSMs. Specifically, the purification and processing of OSMs are outside the scope of this review.

## 2. Recent advances in developing alternative synthetic methods

### 2.1 Atom-economical syntheses – C–H functionalization

The concept of atom economy was first proposed by Trost in *Science* in 1991.<sup>44</sup> The atom economy of a chemical process is measured by the ratio of mass of the desired product to the



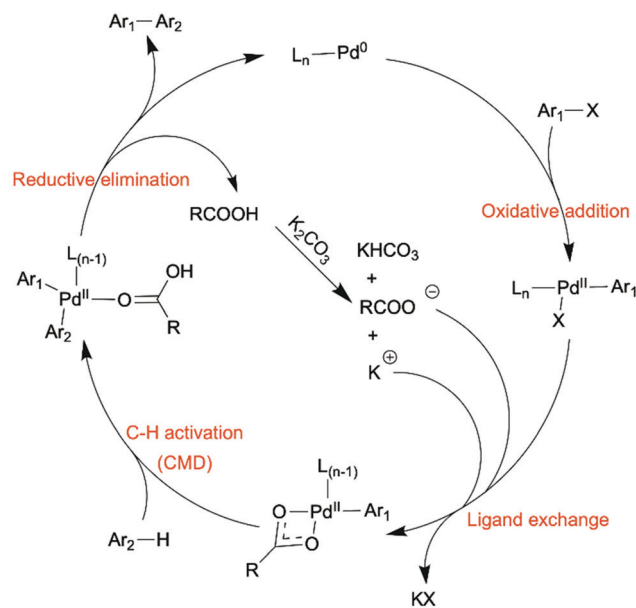


Scheme 2 Comparison among the conventional methods, direct arylation and oxidative C–H/C–H coupling to synthesize OSMs.

total mass of all the products generated, including byproducts. The lower the weight of byproduct(s) a chemical process generates, the more atom-economical the process is. The optimal atom economy is 100%. Reducing the number of steps and avoiding using large functional groups in a synthetic process are effective ways to decrease the generation of wasted byproducts. C–H activation on  $sp^2$  carbons of aromatic rings has become a promising tool to synthesize OSMs, in which the C–H bonds are activated, and subsequently C–C bonds are formed *in situ*. The development of aryl–aryl coupling *via* C–H activation was first driven by pharmaceutical industry, because biaryl structures are very common in many drug compounds. Direct arylation and oxidative C–H/C–H coupling are the two C–H activation involved synthetic routes for OSMs as green alternatives to the conventional synthetic methods, such as Suzuki and Stille couplings, due to their high atom economy (Scheme 2).<sup>29–43</sup> For instance, the atom economy of a Suzuki coupling shown in Scheme 1a is calculated to be 60%. If direct arylation and oxidative C–H/C–H coupling were used instead to synthesize the same organic semiconducting product in Scheme 1a, respectively, then the values of atom economy would be 80% for direct arylation and 99% for oxidative C–H/C–H coupling.

In the direct arylation reaction, only one of the two coupling partners needs to be pre-halogenated, and the necessity of pre-metalation step of the other coupling partner is avoided. Direct arylation has been widely studied as a new method to synthesize OSMs, especially semiconducting polymers.<sup>35,36</sup> Oxidative C–H/C–H coupling, also referred as C–H oxidative direct arylation, is a more ideal synthetic route for OSMs than direct arylation in terms of atom economy, because neither of the coupling partners needs to be pre-functionalized. The unfunctionalized C–H bonds on both coupling partners will be activated and form a C–C bond subsequently during the material synthesis. However, due to the inert nature of C–H bonds, it is more challenging for direct arylation and oxidative C–H/C–H coupling to obtain high-yielding coupling products with desired chemo- and regioselectivity compared to the conventional coupling methods.

**2.1.1 Direct arylation.** Most direct arylation reactions are catalyzed by palladium catalysts in presence of a base, such as  $\text{Cs}_2\text{CO}_3$  and  $\text{K}_2\text{CO}_3$ , and a carboxylic acid which acts as a proton shuttle. Direct arylations are usually carried out under inert gas atmosphere, at an elevated temperature from  $\sim 60^\circ\text{C}$  to  $\sim 120^\circ\text{C}$ , and in aprotic organic solvents such as DMAc, DMF, NMP,



Scheme 3 A plausible catalytic cycle of direct arylation.

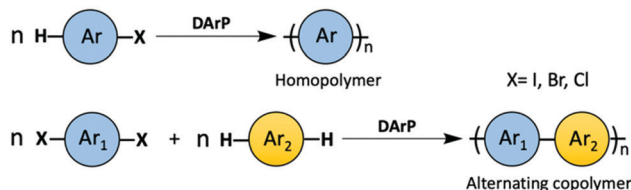
toluene, *etc.*<sup>40</sup> A typical direct arylation catalytic cycle includes the following four major steps (Scheme 3): (i) Oxidative addition, where the Pd(0) catalyst reacts with the C–X bond to form a Pd(II) complex; (ii) Ligand exchange, where X– on the Pd(II) complex is replaced by a carboxylate anion ( $\text{RCOO}^-$ ); (iii) C–H bond activation by the Pd(II) complex; (iv) Reductive elimination to form the C–C bond and regenerate the Pd(0) catalyst.<sup>37,38,40</sup> The C–H activation step in the direct arylation catalytic cycle normally goes through a concerted metalation–deprotonation (CMD) mechanism, and the bases and carboxylic acids are known to assist this process.<sup>45</sup>

In the past few years, most studies using direct arylation to synthesize OSMs focused on synthesizing semiconducting polymers using direct arylation polymerization (DARp). The reports on the synthesis of small molecule organic semiconducting materials *via* direct arylation are less common. Therefore, we will devote a large segment of this section to illustrating some recent advances in semiconducting polymer synthesis by DARp, and briefly discuss about the syntheses of some small molecule OSMs using direct arylation at the end of this section.

DARp, as an emerging subject in the field of OSM synthesis, has been reviewed many times in the past few years.<sup>29–43</sup> The semiconducting polymers synthesized *via* DARp are mostly linear homopolymers and alternating copolymers. When homopolymers are prepared using DARp, the monomer has a C–X ( $\text{X} = \text{Cl}, \text{Br}, \text{I}$ ) bond and a C–H bond to proceed a head-to-tail polycondensation (Scheme 4, top). While, in DARp for alternating copolymers, one of the comonomers is required to possess two reactive C–X bonds and the other comonomer has two C–H bonds (Scheme 4, bottom).

Donor–acceptor (D–A) semiconducting copolymers are very attractive semiconducting materials as their backgrounds demonstrate a “push–pull” mechanism of electron transport. Moreover, these materials display lowered bandgaps, which





Scheme 4 A general scheme of DARp to synthesize semiconducting homopolymer and alternating copolymer.

enables high charge mobility as well as broader ranges for light absorption – useful properties in electronic devices.<sup>1,2</sup> In order to acquire the D–A copolymers with high electronic device performance, the synthesized D–A copolymers need to have perfectly alternating donor and acceptor chemical structures and high molecular weights. Any homo-coupling defect on the polymer backbone limits the material's electronic performance.<sup>46,47</sup> DARp has emerged as a promising and greener synthetic strategy for defect-free D–A copolymers, in contrast to the conventional coupling methods.<sup>48–50</sup>

Synthesizing D–A copolymers *via* conventional coupling methods can be difficult because the pre-functionalization to prepare the required electron-poor comonomers is challenging due to either their unresponsiveness to electrophilic substitution or their decomposition during the functionalization reactions.<sup>51–53</sup> In this case, DARp, where C–H activation of one of the comonomers is a crucial part, appears to be a favorable synthetic method for D–A copolymers. A collaborative work performed by Scott, Luscombe, Marder, and Blakey groups on synthesizing 5,6-dicyano[2,1,3]benzothiadiazole (DCBT)-containing D–A copolymers *via* DARp was reported in 2018.<sup>48</sup> In this work, DCBT was incorporated in D–A copolymers as an electron-poor unit by C–H arylation on DCBT for the first time, and three high molecular weight and perfectly alternating D–A polymers were successfully prepared after condition optimization (Scheme 5a). All three resultant polymers were characterized by broad light absorption and low LUMO levels, and they were proven to be n-type materials for OFET applications with an average mobility of  $1.2 \times 10^{-3} \text{ cm}^2 \text{ V}^{-1} \text{ s}^{-1}$ . Recently, Ozawa *et al.* also reported some syntheses of D–A copolymers with well-defined structures using DARp.<sup>49,50</sup> They prepared a D–A copolymer using 1,2-dithienylethene (DTE) (donor) and dibromoisoidigo (acceptor) as comonomers and a catalytic system consisting of  $\text{Pd}_2(\text{dba})_3 \cdot \text{CHCl}_3$ ,  $\text{P}(2\text{-MeOC}_6\text{H}_4)_3$ , pivalic acid, and  $\text{Cs}_2\text{CO}_3$ .<sup>49</sup> The resulted D–A copolymer exhibited a high molecular weight ( $M_n$  was up to  $44.9 \text{ kg mol}^{-1}$ ) and less than 0.1% homocoupling defect. Moreover, no branching defect was observed, which is important for conjugated polymers containing non-alkylated thiophene as branching and crosslinking, which are results of C–H activation at  $\beta$ -position of thiophene moieties, can lead to the formation of insoluble materials. In addition, the charge transfer properties in OFETs of the D–A copolymer synthesized from DARp was demonstrated to be superior to those of the same D–A copolymer synthesized from Stille coupling. This is likely because the DARp product possessed less structural defect than Stille coupling product and was free of residual tin-containing impurities which

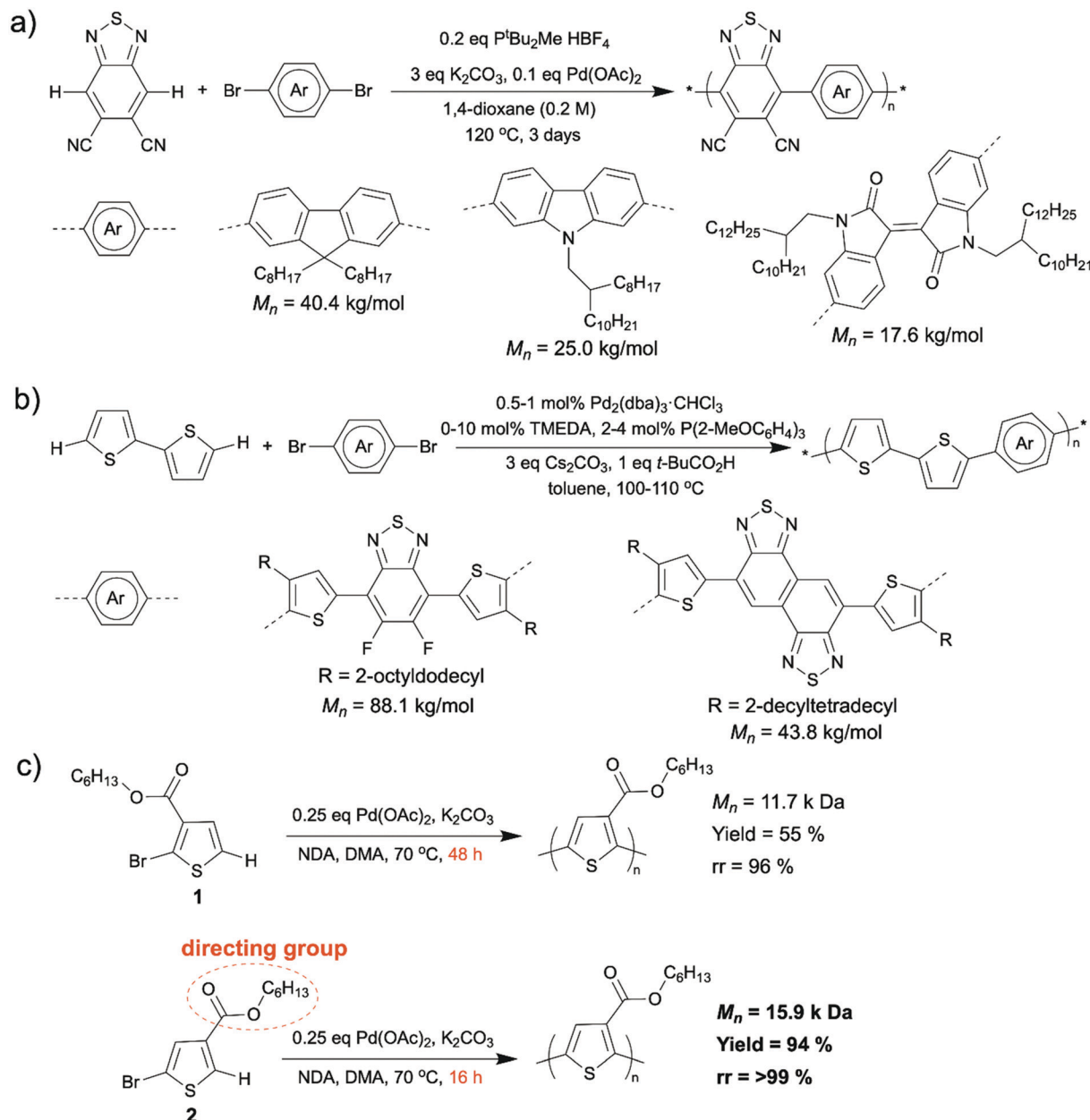
may deteriorate the device performance.<sup>54</sup> In another report published by Ozawa *et al.*, they synthesized D–A copolymers *via* DARp using unsubstituted 2,2'-bithiophene as the donor comonomer without generating insoluble materials (Scheme 5b).<sup>50</sup> In this study, they applied a mixed ligand catalyst ( $\text{P}(2\text{-MeOC}_6\text{H}_4)_3$  and tetramethylethylenediamine (TMEDA) as ligands and  $\text{Pd}_2(\text{dba})_3 \cdot \text{CHCl}_3$  as palladium source) to DARp and successfully suppressed the formation of insoluble materials resulting from branching side reactions. The resulted D–A copolymers displayed high molecular weight (up to  $88.1 \text{ kg mol}^{-1}$ ), low content of homocoupling defects (up to 1.1%), as well as high device performance (power conversion efficiency up to 9.0%).

The control of regioselectivity (head-to-tail) in homopolymer synthesis *via* DARp has always been a big challenge. Activating undesired C–H bonds in DARp can cause structural defects (head-to-head, tail-to-tail, and branching defects) in resultant homopolymers, which diminishes their electronic performance. Utilization of directing groups was demonstrated to be an effectual way to avoid the formation of structural defects during certain DARps. Thompson *et al.* have recently uncovered that using an ester as a directing group installed directly on the thiophene monomer improves the regioregularity (head-to-tail coupling) of the resulted polymer.<sup>55</sup> They installed a hexyl ester directing group adjacent to the C–H bond that was designated for activation on the 2-bromothiophene monomer 2 (Scheme 5c, bottom). Compared to the similar monomer 1 (Scheme 5c, top), where the ester group was installed adjacent to the bromine, the regioregularity of produced poly(3-hexyl ester thiophene-2,5-diyl) (P3HET) improved from 96% to >99%.<sup>56</sup> In addition, the reaction time was reduced from 48 h to 16 h for a similar sized polymer.

DARp normally occurs using a polycondensation mechanism, which is not a controlled polymerization. Conjugated polymers prepared by a polycondensation mechanism will have a broad molecular weight distribution, and the molecular weight can be hard to reproduce. Our group recently achieved chain DARp to synthesize P3HT with a low dispersity.<sup>57</sup> We applied a silver-carboxylate co-catalyst to promote the C–H activation step and PEPPSI-*i*Pr as the palladium source. The association of the polymer chain with the large  $\pi$ -conjugated N-heterocyclic carbene (NHC) ligand on PEPPSI-*i*Pr allowed chain walking of the palladium catalyst along the polymer backbone while adding monomers to the chain ends one by one (Scheme 6). This was also the first report where a dual-catalytic system was implemented in DARp.

In recent years, there have been reports on synthesis of small molecule OSMs using direct arylation. For example, Ching *et al.* successfully applied a two-step synthetic route, direct arylation followed by Knoevenagel condensation, to prepare a new A–D–A–D–A semiconducting small molecule based on benzothiadiazole and thiophene (Scheme 7a).<sup>58</sup> Welch *et al.* published a personal account which summarized their achievements over the last few years in molecule design of organic dye-based non-fullerene acceptors for OPV applications using direct arylation.<sup>59</sup> Direct arylation benefited their research significantly by enabling a facile synthetic access to various molecular structures and easy structural modifications. With this powerful tool, they synthesized





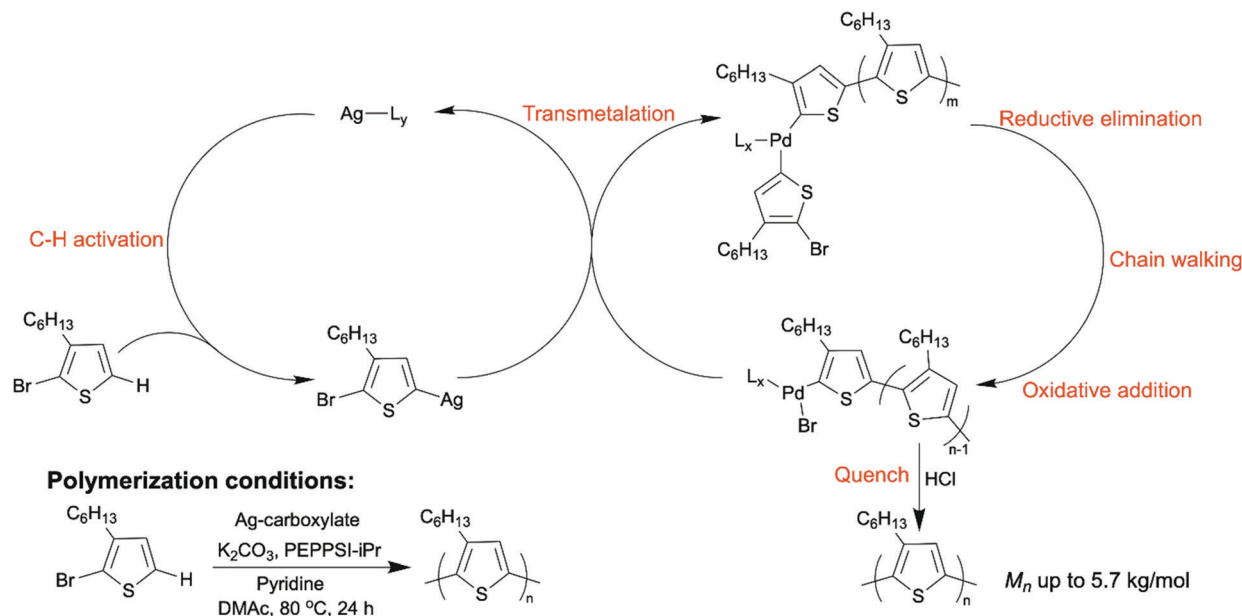
**Scheme 5** (a) Synthesis of DCBT containing conjugated D–A copolymers via DARP. (b) Synthesis of unsubstituted bithiophene containing D–A copolymers via DARP using a mixed ligand catalyst to suppress branching side reactions. (c) Synthesis of highly regioregular P3HET via DARP with the ester functionality as the directing group to promote regioregularity.

isoindigo (ISI)- and diketopyrrolopyrrole (DPP)-based non-fullerene acceptors (Scheme 7b). Perylene diimide–diketopyrrolopyrrole–perylene diimide (PDI–DPP–PDI) was identified as the most promising dye-based framework, the OPV device made from which exhibited a PCE as high as ~6%.<sup>60,61</sup> Our group also reported small molecule organic luminophores with high photoluminescence quantum yields prepared by direct arylation, which will be detailed in the later section.<sup>62</sup>

**2.1.2 Oxidative C–H/C–H coupling.** Oxidative C–H/C–H coupling has received a lot of attention in the organic materials space since its initial report by Fagnou *et al.*<sup>63</sup> In terms of atom economy, it is superior to direct arylation since no pre-halogenation

step is needed. The application of oxidative C–H/C–H coupling towards the OSM synthesis, including small molecule semi-conducting materials, semiconducting homopolymers, and D–A copolymers, have been reviewed considerably in the past few years.<sup>29–34</sup> D–A alternating copolymers are amongst the most challenging semiconducting poly(arylene)s to synthesize *via* oxidative C–H/C–H coupling (also referred to as cross-dehydrogenative coupling (CDC) in this situation) (Scheme 8a), due to the difficulty in achieving high chemo- and regioselectivities when multiple possible reactive sites, in this case C–H bonds, are present. Moreover, the catalysts often have insufficient selectivity to distinguish the donor and acceptor monomers.<sup>63</sup>





Scheme 6 Dual catalytic DARP of P3HT to achieve chain-growth mechanism.

Another challenge when synthesizing D–A copolymers *via* CDC is to obtain high molecular weight polymers. The CDCs are normally driven by the discrepancy in electronic properties of the coupling partners (electron-rich and electron-poor comonomers).<sup>64</sup> The oligomers (dimers, trimers, *etc.*) formed at the beginning of the polymerization are less electron-rich or less electron-poor compared to their corresponding monomers. Therefore, further coupling reactions with these oligomers becomes relatively unfavored, hence inhibiting the chain propagation process that forms long polymer chains.<sup>65</sup> Recent studies have been focused on tackling these issues. Therefore, here we will only discuss the latest advances in D–A copolymer synthesis *via* CDC. In 2018, the Kanbara group and the Chen group both independently reported successful syntheses of highly alternating D–A conjugated poly(arylene)s with large molecular weights *via* CDC for the first time.<sup>66,67</sup>

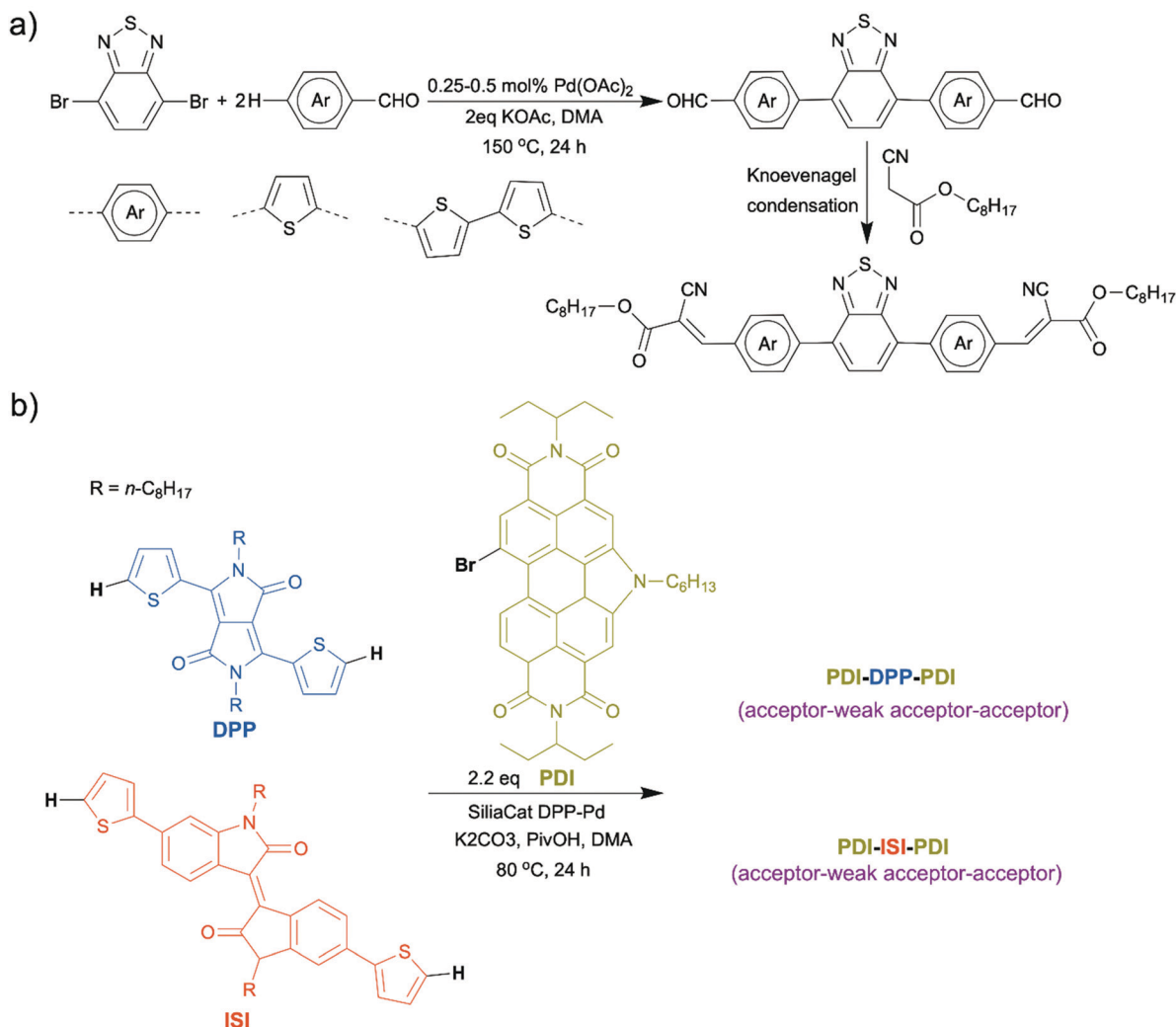
Kanbara *et al.* conducted a palladium/silver dual catalyzed CDC polymerization (Scheme 8b).<sup>66,68</sup> The D–A copolymer they synthesized, a copolymer of 2,2',3,3',5,5',6,6'-octafluorobiphenyl and 3,3'-dihexyl-2,2'-bithiophene, was applied as a light emitting material in OLEDs. Three years later, Lu *et al.* expanded the monomer scope of Kanbara's palladium/silver catalytic CDC polymerization by preparing a series of fluorinated benzotriazole-based D–A conjugated copolymers (Scheme 8c).<sup>69</sup> Chen and co-workers accomplished CDC polymerization of various D–A conjugated copolymers with a similar palladium catalytic system to Kanbara's (Scheme 8d).<sup>67</sup> The highly alternating and regioregular structures of the copolymers were demonstrated by comparing the <sup>1</sup>H NMR spectra of the same copolymers synthesized by Stille coupling, showing the robustness of the CDC method compared to the conventional method.

Our group also published a study on D–A copolymer synthesis *via* a gold/silver catalytic CDC in early 2019.<sup>65</sup> In this study, we attempted to adapt a highly reactive and highly chemo-selective

gold/silver catalyzed small molecule CDC reaction reported by Larrosa into a CDC polymerization.<sup>70</sup> We used the same comonomers as Kanbara did, 2,2',3,3',5,5',6,6'-octafluorobiphenyl and 3,3'-dihexyl-2,2'-bithiophene. The resulted copolymers showed low molecular weights (7.5 kg mol<sup>-1</sup>) and ~70% degree of alternation, but we gained a great insight into the factors that determine the chemo-selectivity and readiness of chain propagation during the CDC polymerization, which were mentioned in the early discussion about the challenges in D–A copolymer synthesis *via* CDC.

Apart from poly(arylene)s, another type of promising semi-conducting polymers which was successfully synthesized *via* oxidative C–H/C–H coupling are luminescent poly(arylene–vinylene)s (Scheme 9a).<sup>71–73</sup> In 2016, the Kanbara group depicted the first oxidative C–H/C–H polymerization of a diethenyl aromatic monomer and an arene monomer, namely dehydrogenative direct alkenylation polycondensation, to synthesize several 1-(2-pyrimidinyl)pyrrole-based poly(arylene–vinylene)s with a rhodium catalyst (Scheme 9b, top).<sup>71</sup> After that, they reported a palladium catalyzed dehydrogenative direct alkenylation polymerization of polyfluoroarylene-based poly(arylene–vinylene)s (Scheme 9b, bottom).<sup>72</sup> In this report, they eliminated the necessity of installing the directing 2-pyrimidinyl group. This year, they published a synthesis of 1-(2-pyrimidinyl)pyrrole-based poly(arylene–vinylene)s from aromatic diynes by polyaddition *via* a cobalt-catalyzed hydroarylation of alkynes (Scheme 9c).<sup>73</sup> Technically this does not fall into the oxidative C–H/C–H coupling category since it is an addition reaction instead of condensation, discussed here for its extraordinary atom-economy (no byproducts), enriching the toolbox of green synthesis for OSMs. Although the polymers that were synthesized *via* the polyaddition contained a small number of 1,1-vinylidene units (7%), which are problematic for using these materials in electronic devices, this cobalt-catalyzed dehydrogenative polyaddition is still very appealing because it proceeded at near





**Scheme 7** (a) Synthesis of small molecule OSMs via direct arylation. (b) Synthesis of isoindigo (ISI)- and diketopyrrolopyrrole (DPP)-based non-fullerene acceptors via direct arylation.

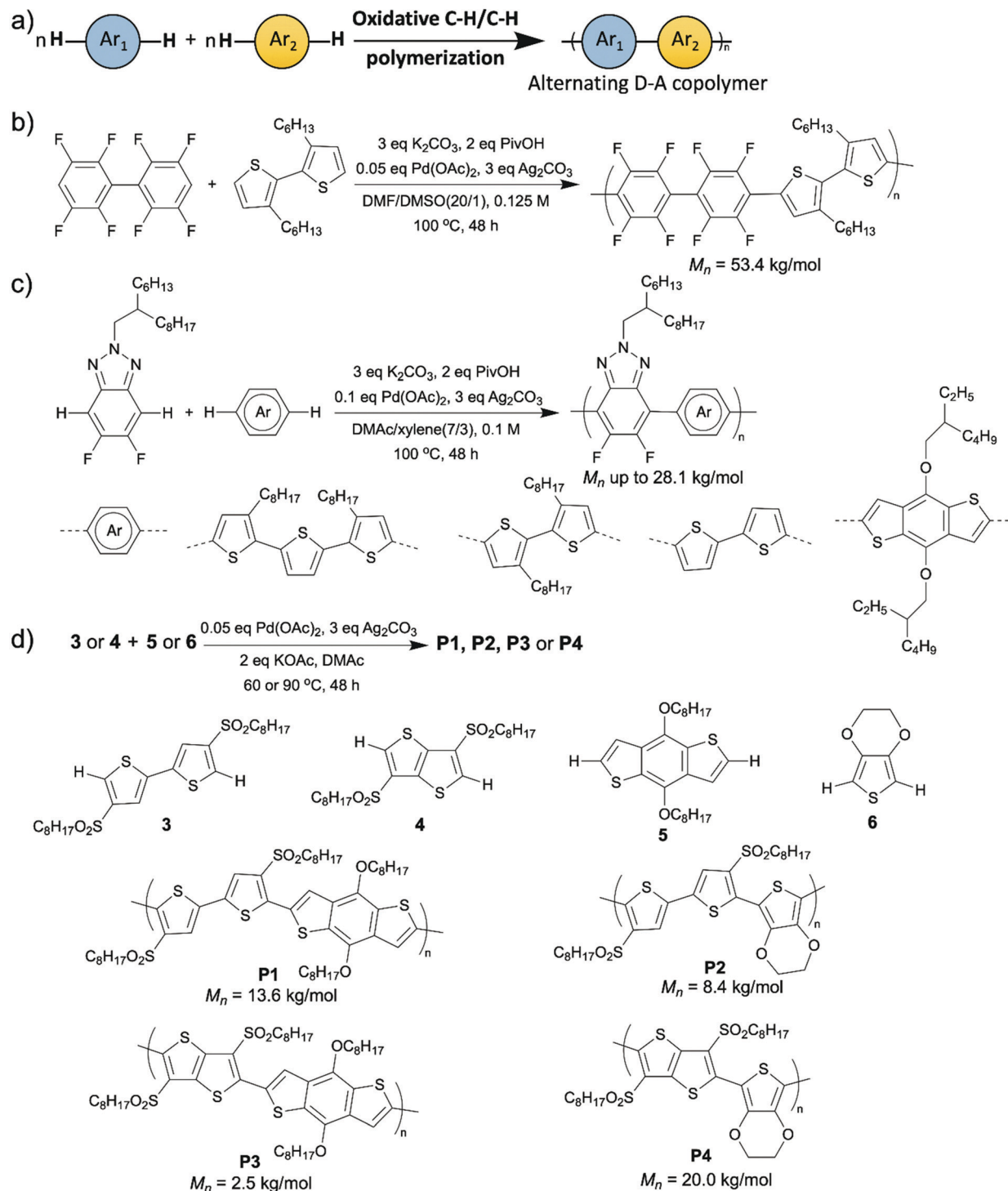
room temperature (30 °C), avoided using stoichiometric amounts of oxidants, and applied a first-row transition metal (cobalt) catalyst.

## 2.2 Energy-efficient conditions in atom-economical syntheses

Minimizing energy input in the synthetic process of OSMs is an important part of improving the environmental friendliness and scalability of OSM production. As we discussed before, most atom-economical synthetic methods (direct arylation and oxidative C–H/C–H coupling) for OSMs are carried out under inert atmosphere and at relatively elevated temperatures (~60 °C to ~120 °C). Conducting the synthetic reactions at room temperature can lessen the thermal energy that were put into the OSM production significantly. In addition, a mild reaction temperature can also lower the risk of dangerous accidents during manufacturing. The synthetic reactions that can tolerate the aerobic conditions can avoid the long and energy-intensive degassing processes to remove moisture and oxygen. Moreover, commercially available and cheap reagent-grade chemicals can be directly used for the moisture- and oxygen-tolerant reactions.

The reports on room-temperature synthesis of OSMs are not very common compared to those on optimizing other aspects of OSM synthesis, such as additives, catalysts, and solvents. This is likely because when the C–H bond, which is less reactive than other organometallic functionalities, needs to be activated, the introduction of an external energy source, such as heat, or employment of highly reactive additives is usually required.<sup>74</sup> The first attempt to synthesize OSMs by room-temperature DARp was reported by Thompson *et al.*<sup>75</sup> They prepared P3HT using DARp at 20 °C and obtained a polymer with a molecular weight of 14 kg mol<sup>-1</sup> but a low yield of only 9%. To our knowledge, the second attempt to achieve room-temperature DARp was made recently by our group. In this study, we synthesized a low molecular weight and branched semiconducting homopolymer from 5-iodo-1-octylindole monomer using room-temperature DARp as shown in Scheme 10.<sup>76</sup> Notably, the mechanistic study indicated that this polymerization was governed by a light-mediated radical process, which was a significant discovery that can inspire future developments of mild reaction conditions for





**Scheme 8** (a) A general synthetic scheme of D–A semiconducting copolymers *via* CDC. (b) Palladium/silver catalyzed CDC polymerization. (c) Synthesis of fluorinated benzotriazole containing D–A conjugated copolymers *via* CDC. (d) The CDC polymerizations of various D–A conjugated copolymers.

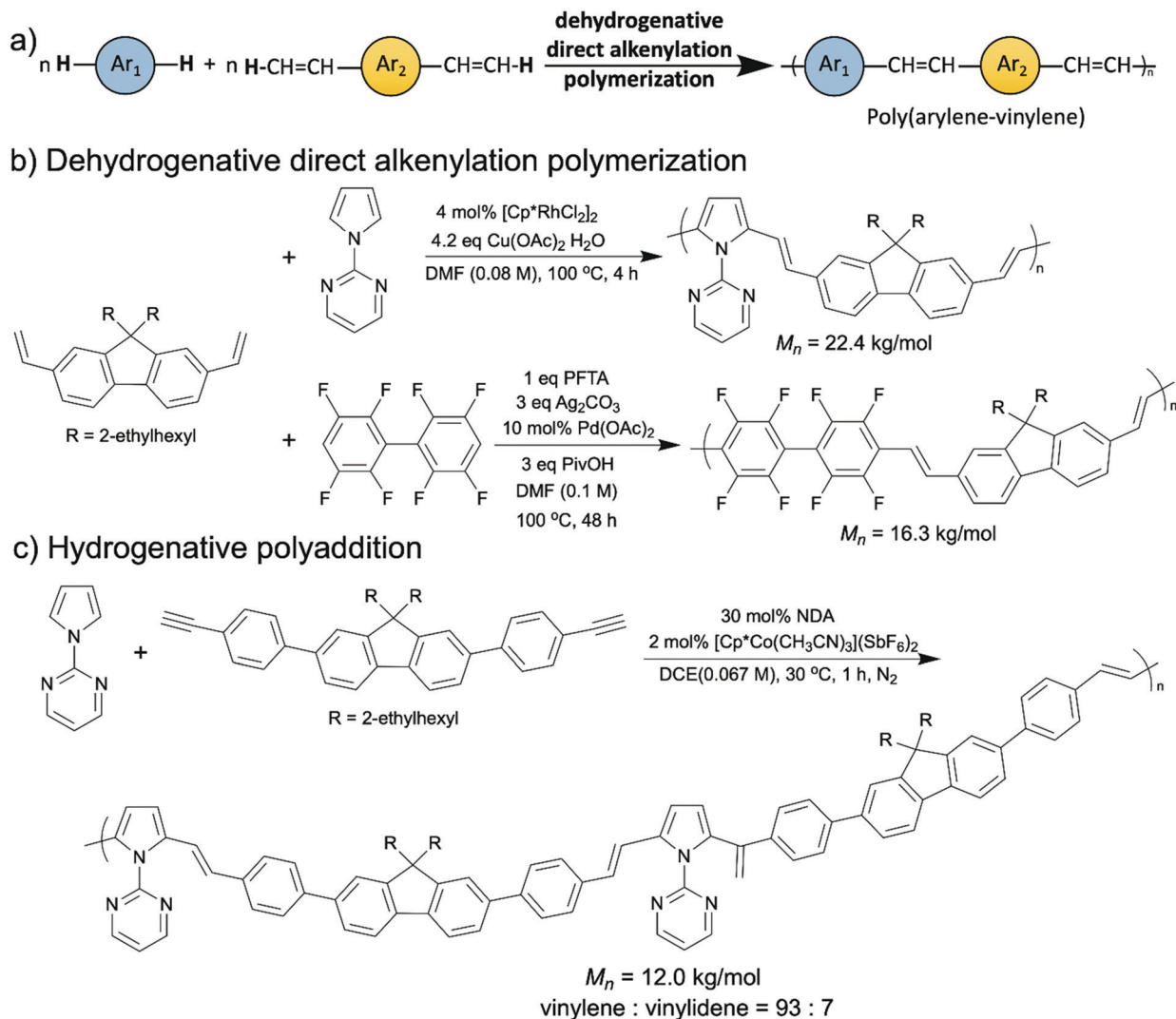
DARF. Also, the aforementioned polyaddition *via* a cobalt-catalyzed hydroarylation of alkynes reported by Kanbara group is another example of near room temperature synthesis of OSMs.<sup>73</sup>

Direct arylation and oxidative C–H/C–H coupling are usually performed under inert gas because most of their catalysts and generated intermediates are air and moisture sensitive.<sup>77,78</sup> In

recent years, Kanbara *et al.* discovered that refluxing the solvent (toluene, *o*-xylene, or DMF) during the polymerization allows certain DARF reactions to proceed under aerobic conditions.<sup>79,80</sup> The aerobic DARF of 5-(2-ethylhexyl)thieno-[3,4-*c*]-pyrrole-4,6-dione (TPD) with 2,7-dibromo-9,9-dioctylfluorene was accomplished in the refluxed toluene with a molecular weight up to







Scheme 9 (a) A general scheme of dehydrogenative direct alkenylation polymerization to synthesize poly(arylene-vinylene)s. (b) Rhodium- and palladium catalyzed dehydrogenative direct alkenylation polymerizations to synthesize poly(arylene-vinylene)s. (c) Cobalt-catalyzed hydrogenative polyaddition to synthesize poly(arylene-vinylene)s.



Scheme 10 Room-temperature DARp of 5-iodo-1-octylindole monomer.

176.8 kg mol<sup>-1</sup>.<sup>79</sup> In their other report, a copolymer of 3,4-ethylenedioxythiophene (EDOT) and 2,7-dibromo-9,9-dioctylfluorene with a molecular weight of 54.2 kg mol<sup>-1</sup> was successfully synthesized *via* DARp under aerobic conditions by refluxing the solvent DMF.<sup>80</sup> The authors attributed this to efficient degassing of dissolved oxygen from the reaction mixture and prevention of resolubilizing oxygen.<sup>79,80</sup> Aside from DARp, the Kanbara group also reported a few oxidative C-H/C-H polymerizations carried out under aerobic conditions. In the same paper where they achieved the initial oxidative

C-H/C-H polymerization to synthesize D-A copolymers, they were able to conduct the same polymerization under aerobic atmosphere as well, obtaining a D-A copolymer with high molecular weight (23.2 kg mol<sup>-1</sup>) and only 2% homo-coupling defects.<sup>66</sup> In the same year, their study of copper-catalyzed aerobic oxidative C-H/C-H homo-polymerization of dithiazole-based monomer was published, where dioxygen acted as the oxidant.<sup>81</sup> Notably, a copper catalyst was applied in this polymerization, which made this polymerization protocol better than other palladium catalyzed ones in terms of environmental friendliness. This will be detailed in the Section 2.3.2.

### 2.3 Safe and abundant chemicals for atom-economical syntheses

**2.3.1 Green solvents.** The impact of the chemicals used for OSM synthesis on human health and the environment is a crucial measurement for understanding environmental friendliness of OSM production. Among the chemicals that are added in a chemical transformation, solvents are usually used in the largest quantity. Consequently, optimizing the solvents is one of the most



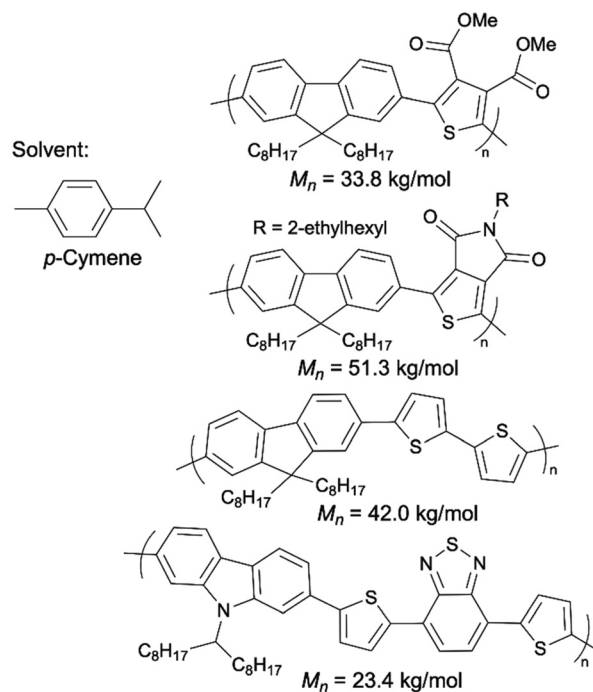
effective ways to improve the greenness of the chemicals used in OSM synthesis. A solvent can be identified as green and safe if it has low or no toxicity to humans and the environment, requires low energy to produce, and is naturally abundant, namely agrees with the 12 Principles of Green Chemistry.<sup>42,82,83</sup> According to this standard, water should be the safest and greenest solvent that exists so far. However, it is not easy to perform an organic reaction in water as most organics are insoluble in water. The organic solvents that are extensively used in the synthesis of OSMs are mostly aprotic solvents, including DMF, toluene, THF, chlorobenzene, *etc.*<sup>33,34,40,42</sup> These solvents are favored in OSM synthesis not only because of the high solubility of the organic starting materials and semiconducting products in them, but also because solvents such as DMF and DMAc can act as ligands coordinating to the metal complexes in the reactions.<sup>34,38</sup> Unfortunately, these organic solvents are typically highly hazardous to humans and the environment, which makes them unsuitable from an environmental perspective.<sup>84</sup> Yet, there are relatively greener and more sustainable organic solvents that have been proven to be amenable to organometallic reactions. These solvents can be produced and used in large quantities without damaging the environment and human health because they are biomass-derived, for example 2-methyltetrahydrofuran (2-MeTHF),  $\gamma$ -valerolactone (GVL), diethyl carbonate (DEC), and cyclopentyl methyl ether (CPME), *etc.*<sup>42,85–89</sup> In this section, the latest progress in development of OSM synthesis in green solvents will be reviewed.

Thompson and colleagues conducted a solvent optimization for the DArP of poly[2,5-bis(2hexyldecyloxy)phenylene-*alt*-(4,7-dithiophen-2-yl)benzo[*c*][1,2,5]thiazole] (PPDTBT) synthesis using the four green organic solvents aforementioned.<sup>90</sup> Among these solvents, CPME gave preminent results. The molecular weight of PPDTBT synthesized in CPME was measured to be 41 kg mol<sup>-1</sup> by size exclusion chromatography (SEC), which surpassed the previously reported PPDTBT prepared under THF conditions (15 kg mol<sup>-1</sup>). In addition, they also performed DArP to synthesize P3HT in CPME, which provided a P3HT with the molecular weight of 12 kg mol<sup>-1</sup> and regioregularity of 93%. Grisorio, *et al.* also investigated the possibility of using another sustainable solvent, anisole in DArP to synthesize P3HT.<sup>91</sup> Anisole is a low-cost, non-toxic, biodegradable, and highly recommended organic solvent based on recent solvent selection guides.<sup>92</sup> The best P3HT they obtained was endowed with the molecular weight of 17.2 kg mol<sup>-1</sup> and regioregularity of 93%. Thompson and colleagues reported more syntheses of other semiconducting polymers *via* DArP performed in green solvents.<sup>93,94</sup> They used anisole and CPME in the synthesis of diester functionalized bithiophene-containing polymers, poly[5,5'-bis(2-butyloctyl)-(2,2'-bithiophene)-4,4'-dicarboxylate-*alt*-5,5'-2,2'-bithiophene] (PDCBT) (13.8 kg mol<sup>-1</sup>), poly[5,5'-bis(2-butyloctyl)-(2,2'-bithiophene)-4,4'-dicarboxylate-*alt*-2,5-[3,2-*b*]thienothiophene] (PDCTT) (26.4 kg mol<sup>-1</sup>), and poly[5,5'-bis(2-butyloctyl)-(2,2'-bithiophene)-4,4'-dicarboxylate-*alt*-5,5'-2,2'-bithiazole] (PDCBTz) (4.9 kg mol<sup>-1</sup>).<sup>93</sup> They also synthesized a series of amide-functionalized semiconducting polymers using CPME.<sup>94</sup>

2-MeTHF is a popular green alternative to THF. Pappenfus *et al.* successfully scaled up P3HT synthesis to 10 g *via* DArP solvated by 2-MeTHF.<sup>95</sup> The P3HT prepared in 2-MeTHF exhibited

a molecular weight of 22.8 kg mol<sup>-1</sup>, high regioregularity, and zero  $\beta$ -branching defects. Recently, Thompson introduced a new, naturally sourced aromatic solvent, *p*-cymene, for DArP as a green alternative to toluene and xylenes.<sup>96</sup> *p*-Cymene is a side product generated in large quantities in citrus fruit processing.<sup>97</sup> They demonstrated that *p*-cymene outperformed toluene, DMA, and THF in the synthesis of some D-A copolymers using DArP (Scheme 11).

Lately, there are also some exciting breakthroughs in OSM preparation in water. In 2017, Leclerc *et al.* developed water/toluene (1/1) biphasic DArP conditions for the synthesis of a wide range of semiconducting polymers (thienyl and phenyl-based) without reducing the polymer molecular weight and other important properties, which is the first example where water was used as a co-solvent for DArP.<sup>98</sup> In their research, tetrabutylammonium chloride (TBAC) was added as phase transfer agent. Delightfully, their water/toluene biphasic DArP was also demonstrated to be air tolerant. In 2018, Yu *et al.* reported DArPs to synthesize water-soluble alkoxy-sulfonate- and carboxylic acid-functionalized poly(3,4-ethylenedioxythiophene)s (PEDOTs) in DMF and water, respectively.<sup>99</sup> Tetrabutylammonium bromide (TBAB) was used a phase transfer agent in the water solvated DArP. The DArP conducted in water provided a PEDOTS polymer with molecular weight of 6.4 kg mol<sup>-1</sup> and a yield of 80%. In 2020, Liu group reported an aqueous DArP to prepare water-soluble semiconducting polymers from ammonium bromide- and sulfonate-functionalized thiophene monomers, 6-(2-(2-bromothiophen-3-yl)ethoxy)hexyl trimethylammonium bromide and 4-(2-(2-bromothiophen-3-yl)ethoxy)butylsulfonate.<sup>100</sup> The molecular weights were up to 10.0 kg mol<sup>-1</sup>.



Scheme 11 Semiconducting polymers synthesized by DArP with *p*-cymene as the solvent.

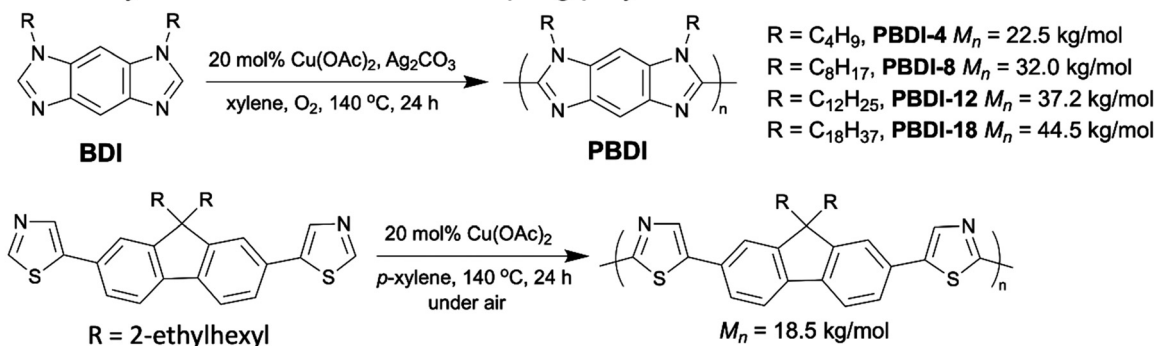


**2.3.2 First-row transition-metal catalysts.** Noble transition-metals, such as palladium, rhodium, ruthenium, and iridium, are heavily used in most coupling methods (including direct arylation and oxidative C–H/C–H coupling) for OSMs as catalysts, especially palladium due to its broad ligand scope.<sup>38,101–103</sup> These noble transition-metals are not only expensive and unsustainable but also toxic. Hence, the residual metal in the final products prevent the utilization of the OSMs involving these noble transition-metals in biomedical applications.<sup>104</sup> To lessen the environmental

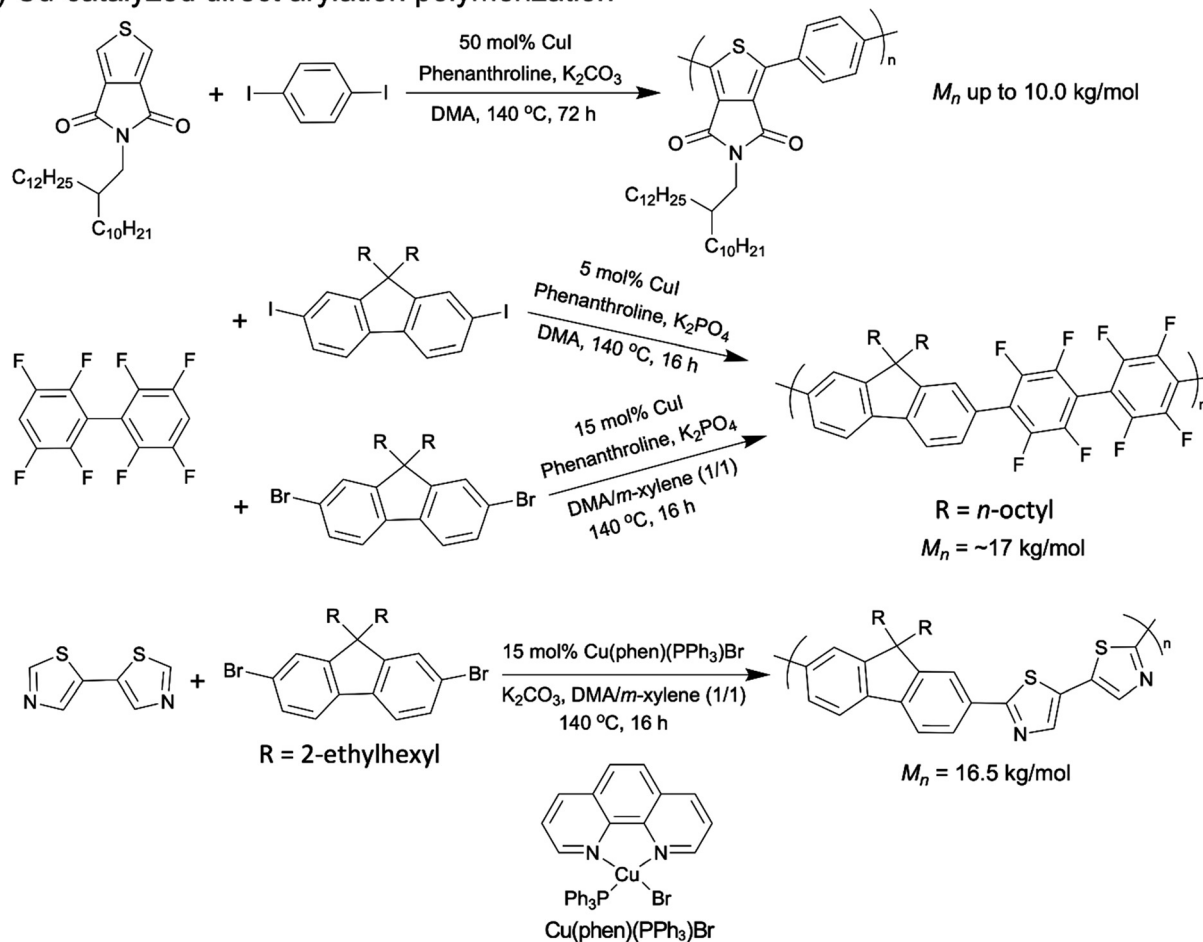
risk of OSM synthesis and extend the range of OSM application, developing atom-economical synthetic pathways catalyzed by less toxic, more earth-abundant, and more biocompatible first-row transition-metals (*e.g.*, iron, cobalt, nickel, and copper) is imperative.

Although the investigations into replacing noble transition-metals with environmentally benign first-row transition-metals in OSM synthesis emerged decades ago, challenges remain in first-row transition-metal catalyzed direct arylation and oxidative C–H/C–H coupling. Thus far, among the first-row

### a) Cu-catalyzed oxidative C–H/C–H coupling polymerization



### b) Cu-catalyzed direct arylation polymerization



Scheme 12 (a) Cu-catalyzed oxidative C–H/C–H coupling polymerizations. (b) Cu-catalyzed direct arylation polymerizations.



transition-metals, only copper was successfully applied as a catalyst in DARp and oxidative C–H/C–H polymerization. However, the monomers in the copper-catalyzed C–H polymerizations are often limited to nitrogen-containing heterocycles, such as thiazole, oxazole, and imidazole. This is because the nitrogen atoms are good coordinating sites to the copper-center, and by coordinating to the copper-center, the energy barrier to activate the adjacent C–H bonds can be decreased.<sup>105</sup> In this section, we will summarize all the copper catalyzed DARps and oxidative C–H/C–H coupling polymerizations that have been published so far.

The first OSM synthesis *via* copper catalyzed oxidative C–H/C–H polymerization was reported by the You group in 2014. Various regioregular polybenzodiimidazoles (PBDIs) were prepared with the 20 mol% copper catalyst (Scheme 12a, top).<sup>106</sup> The PBDIs they obtained exhibited high regioregularity and were blue emitters. Afterwards, at the beginning of 2018 Kanbara *et al.* published the second example of copper catalyzed oxidative C–H/C–H coupling polymerization using a dithiazole-based monomer with between 10–20 mol% catalyst loadings, which was mentioned in section 2.2 (Scheme 12a, bottom).<sup>81</sup>

The above two examples are restricted to homo-polymerization of nitrogen-containing heterocyclic monomers. Thompson and colleagues published a series of studies on copper catalyzed DARp to synthesize D–A copolymers.<sup>107–110</sup> The first copper catalyzed DARp for D–A copolymer synthesis was reported in 2018 by Thompson. Thieno[3,4-*c*]pyrrole-4,6-dione (TPD)-containing D–A copolymers were prepared with the catalyst loading of 50 mol% and the molecular weights of  $\sim 4\text{ k}$  to  $\sim 10\text{ k g mol}^{-1}$  (Scheme 12b, top).<sup>107</sup> In the same year, they achieved a synthesis of a D–A copolymer of fluorene and fluoroarenes ( $M_n = 16.4\text{ k g mol}^{-1}$ ) *via* DARp by employing only 5 mol% copper catalyst (Scheme 12b, middle).<sup>108</sup> The above two examples of copper catalyzed DARp both required the use of aryl iodides as the comonomers whose preparation processes are normally more challenging and less sustainable than those of aryl bromides.<sup>111</sup> Thus, in their next report on copper catalyzed DARp in 2019, they developed a new catalytic system for aryl-bromides, which led to the same fluorene-fluoroarene copolymer with a good molecular weight of  $17.3\text{ k g mol}^{-1}$  (Scheme 12b, middle).<sup>109</sup> It is worth noting that the only modification they made to accomplish the copper catalyzed DARp for aryl bromides was the solvent. In the new catalytic system for aryl-bromides, a DMA/*m*-xylene (1/1) co-solvent system was adopted, while in the DARp for aryl iodides the solvent was DMA solely. In 2020, Thompson and colleagues further upgraded their copper catalyzed DARp for aryl bromides by substituting the original CuI catalyst with a soluble and stable Cu(I) pre-catalyst, Cu(phen)(PPh<sub>3</sub>)Br.<sup>110</sup> With the new copper catalyst, they synthesized a fluorene and dithiazole-based D–A copolymer with molecular weight of  $16.5\text{ k g mol}^{-1}$  within 16 h (Scheme 12b, bottom).

### 3. Naturally sourced building blocks for OSM syntheses

One of the attempts to reduce the harm of a synthetic process to the environment is to use naturally sourced products as the

building blocks and develop synthetic protocols that mimic the naturally occurring processes.<sup>112</sup> Naturally occurring products and processes are innocuous and compatible to the environment. In addition, most natural organic chemicals are intrinsically biocompatible, bio-renewable and biodegradable.<sup>113,114</sup> Whereas, as discussed in the introduction, the current building blocks of OSM, such as thiophene, are mostly toxic and often produced by environmentally harmful and energy intensive synthetic procedures. Shifting the building blocks of OSMs to these environmentally compatible and benign natural products is conducive to enhancing the environmental friendliness of OSMs. Herein, we advocate three promising naturally sourced organic materials that have displayed potential to be applied as OSMs and OSM building blocks, while being non-toxic to humans. They are indigo, melanin, and caffeine analogues.

#### 3.1 Indigo

Indigo (2,2'-bis(2,3-dihydro-3-oxoindolyden)) is a cheap natural blue dye (a few USDs per kg) with a rich history of at least 6000 years. It was initially obtained from indigo plants (*Indigofera tinctoria*, *Indigofera suffruticosa*, *Isatis tinctoria*, etc.). Its major application is dyeing denim cloth and blue jeans. Although indigo is now primarily produced synthetically with a one-pot Heumann–Pfleger reaction on large industrial scales,<sup>115</sup> its environmental compatibility (non-toxicity, biocompatibility, and biodegradability) still allows it to be considered a relatively green building block for OSMs. It was in 2006 that the use of indigo and its derivatives as OSMs was initially proposed in a Japanese patent.<sup>116</sup> Since then significant efforts towards incorporating indigo in the organic electronics have emerged.<sup>115,117–130</sup>

Indigo has exhibited very promising semiconducting behaviors. It has balanced ambipolar charge transport, stemming from its reversible redox states and displays good charge mobility ( $1 \times 10^{-2}\text{ cm}^2\text{ V}^{-1}\text{ s}^{-1}$ ).<sup>115,117</sup> The intra- and intermolecular hydrogen bonding between N–H and C=O groups contributes to the high charge mobility of indigo. Intramolecular hydrogen bonding results in a highly trans-planar structure, which allows extensive delocalization of electrons (Scheme 13a). The intermolecular hydrogen bonding leads to the indigo molecules tightly stacking together, which explains high crystallinity of indigo thin films formed on aliphatic nonpolar substrate upon vacuum evaporation.<sup>115,117,118</sup> Indigo thin films have been extensively used in OFET devices, organic inverters, and photodiode as active layers.<sup>117–121</sup> Indigo is electronic deficient and has been used as a non-fullerene acceptor in blends with the donor P3HT for use in OPVs.<sup>122</sup> Besides acting as a small molecule semiconductor itself, indigo is also an electron accepting building block in semiconducting D–A copolymers.<sup>123–126</sup> Indigo is a striking OSM or a OSM building block not only because of its excellent optical and electronic properties, but also because it is non-toxic, air stable, biocompatible, and biodegradable, enabling its applications in the biomedical field.<sup>131,132</sup>

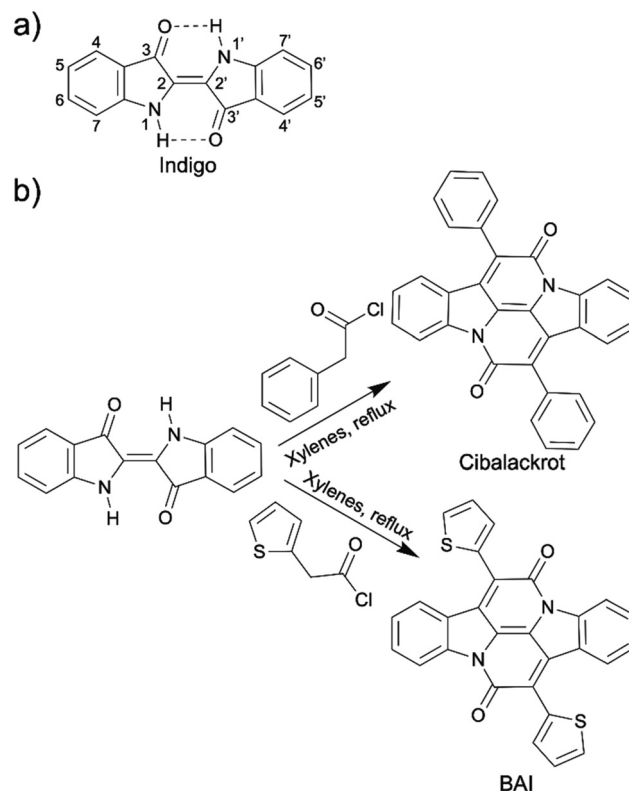
Indigo, however, has very poor solubility in organic solvents owing to its hydrogen bonds, which prevents it from being



solution processible like some of other OSMs. The poor solubility of indigo in organic solvents also limits the synthetic chemistry using indigo as a starting material. Functionalizing the indigo molecule with solubilizing groups is an applicable approach to improving its solubility. However, carelessly attaching any solubilizing functional groups to random positions on indigo molecule may cause distortion of the planarity of the molecule, which will hamper its charge mobility. For example, in the work on synthesis of indigo-based D–A copolymers by Li *et al.*, their indigo monomer had an acyl side chain as the solubilizing group, which led to twisted polymer backbones in the produced D–A copolymers and reduced effective main chain conjugation length.<sup>123</sup>

One of the most effective ways to improve solubility of indigo without harming its electronic properties is to disrupt the hydrogen bonding reversibly, which is so called protection–deprotection. Before processing or reactions, a photo-, acid-, and/or thermo-labile protection group, for example *tert*-butoxy carbonyl (*t*BOC) group, has been attached to the nitrogen atom on the indigo to break the inter-molecular hydrogen bonding temporarily, which makes the protected indigo soluble. After the solution processing or chemical reactions, light, heat and/or acid treatment can be carried out to deprotect and regenerate the indigo or indigo moieties.<sup>122,124,125</sup> However, this method is not flawless. The solution processed indigo thin films after deprotection have contained large hydrogen-bonded crystallites, causing morphological defects (rough and discontinuous films).<sup>122</sup> In addition, the protection and deprotection are extra steps in the synthetic/fabrication processes, which does not help with atom-economy. There is also work that has been done to improve the solubility of indigo without interrupting the N–H and C=O hydrogen bonding. Recently, the Li group reported a synthesis of a D–A copolymer using an indigo-based monomer with a long alkoxy solubilizing group (2-octyldodecyloxy) attached to the 7,7'-positions.<sup>126</sup> Although the synthesized polymer displayed the highest hole mobility (up to 0.016 and 0.028 cm<sup>2</sup> V<sup>-1</sup> s<sup>-1</sup>) for indigo-based polymers and was demonstrated to be an excellent material for OFET based fluoride sensors, the synthetic route for this polymer contained five steps and four of them are for synthesizing the functionalized indigo monomer alone.

Another practical solution to the insolubility of indigo is to replace the intra-molecular N–H and C=O hydrogen bonding with annulated rings, which not only reinforce the coplanarity of the chemical structure but also opens up another electron conducting direction that is nearly orthogonal to the original conducting direction of indigo (Scheme 13b). This annulated indigo was first synthesized in 1914 from indigo and phenylacetyl chloride. The product was called cibalackrot.<sup>133</sup> In 2014, instead of reacting indigo with phenylacetyl chloride, Liu *et al.* synthesized an annulated indigo from 2-thienylacetyl chloride, which is named bay-annulated indigo (BAI) because the annulation occurs at the bay positions on the indigo.<sup>134</sup> Delightedly, these annulated indigos only take one step to synthesize from indigo and thiopheneacetyl or phenylacetyl chlorides. The solubility of them was slightly improved compared to indigo because hydrogen bonding was removed, but it is still relatively low due to strong



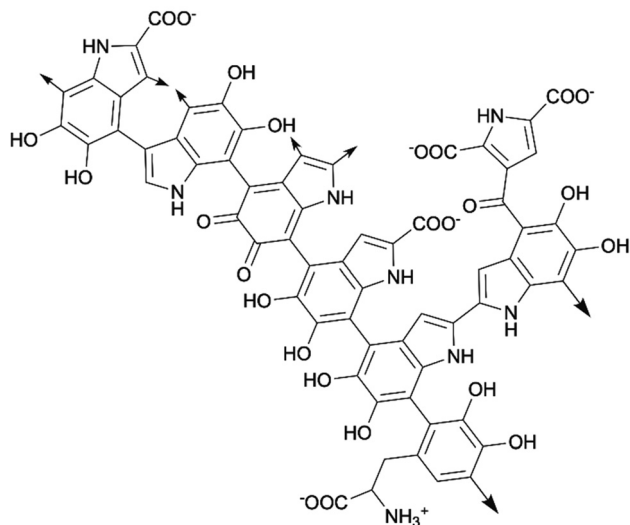
Scheme 13 (a) Chemical structure of indigo. (b) Annulation reaction of indigo to synthesize cibalackrot and BAI.

$\pi$ - $\pi$  interaction. Nevertheless, annulated indigos have more suitable functionalization sites for installation of a solubilizing group without sacrificing their electronic properties compared to indigo. Another strategy is to pre-install the solubilizing group (alkyl chain) on the thiopheneacetyl or phenylacetyl chloride before the annulation reaction.<sup>135,136</sup> The applications of cibalackrot and BAI as organic OSMs or OSM building blocks have been shown in many organic electronic fields, such as OPVs, OFETs, organic lasers, and OLEDs.<sup>135–138</sup>

### 3.2 Melanin

The term “melanin” represents a class of polymeric natural pigments, which are ubiquitously present in animals such as bird feathers, cuttlefish ink, insect exoskeletons, human skin, and even in human brains. They are highly biocompatible and biodegradable. Some melanin macromolecules can also be found in wounded plant tissues and microorganisms. Naturally occurring melanin consists of five basic types: eumelanin, pheomelanin, allomelanin, pyomelanin, and neuromelanin.<sup>139,140</sup> At present, when most researchers talk about melanin, they are referring to the black-brown eumelanin, which is the most common and easy to access type of natural melanin.<sup>141</sup> Although the existence of melanin was discovered in 19th century, the exact chemical structure has always been debated due to its complexity. Generally, melanin macromolecules are extensively conjugated two-dimensional polymeric sheets that are primarily composed of 5,6-dihydroxyindole (DHI), 5,6-dihydroxyindole-2-carboxylic





Scheme 14 Part of chemical structure of two-dimensional melanin sheet (arrows means the positions where the sheet could extend from).

acid (DHICA), and their redox derivatives.<sup>142</sup> The biosynthesis of melanin *in vivo* happens in melanocyte cells, starting with oxidation of tyrosine which gives DHI and DHICA. Then the polymerization occurs to form melanin. The synthesis of melanin *in vitro* is mostly done by oxidating tyrosine with hydrogen peroxide, followed by polymerization.<sup>143</sup> The melanin synthesized *in vitro* is called synthetic melanin. Melanins generated from different sources or environments have different contents of each subunit, resulting in melanin's irregular chemical structure. A generic chemical structure of part of melanin is shown in Scheme 14.<sup>139,142</sup>

Melanin, as a natural biomaterial, has a broadband light absorption range, spanning across the UV, visible, and near-infrared (NIR) regions. In addition, melanin has multiple bandgaps ranging from 2.0 to 3.7 eV because of the complex nature of its chemical structure.<sup>144,145</sup> The outstanding optical property of melanin is associated with its photoprotective function in human skin. In 1970s, McGinness *et al.* as well as Powell and Rosenberg reported the electrical conductivity of melanin, which unlocked the applications of melanin in organic electronic field.<sup>146,147</sup> It was found that melanin is amorphous in the solid state due to the irregularity of its chemical structures. McGinness *et al.* proposed that the origin of charge transport in melanin was explained by the amorphous semiconductor model.<sup>146</sup> However, around 40 years later Mostert *et al.* showed evidence pointing that the melanin was a hybrid ionic–electronic semiconductor instead of a typical amorphous semiconductor, and the charge carriers in melanin were electrons and protons.<sup>148,149</sup> The optical and electronic properties have made melanin a great OSM for OPV,<sup>150,151</sup> OLED,<sup>152</sup> and other optoelectronic applications.<sup>153</sup> The hybrid ionic–electronic conductivity endowed melanin with a prominent position in organic electrochemical transistors (OECT).<sup>154,155</sup> It is worth mentioning that the electrical conductivity of melanin strongly and positively correlates to its hydration state,<sup>146,147</sup> enabling melanin's application in humidity sensors.<sup>156,157</sup> It can also be used as a pH sensor,

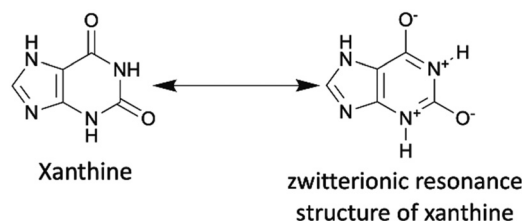
ascribed to the H<sup>+</sup> ion binding ability of carboxylate groups in melanin.<sup>158</sup> The viability of melanin as implanted bioelectronics has also been examined.<sup>159,160</sup> Moreover, there are reports showing the potential of melanin to be used in batteries.<sup>161–163</sup> The applications of melanin as an OSM was also carefully reviewed by Shankar *et al.*<sup>142</sup>

Compared to indigo, developments of organic electronics using melanin are still in its early stages. There are two major barriers remaining. One is the industrial scalability limited by the scarcity of melanin. The most common natural source of melanin is from animals, specifically cuttlefish ink, which is not as accessible as plant-derived chemicals. This leads to the high price of commercially available melanin which according to Sigma-Aldrich is 464.00 USD per gram in 2021. It is imperative for the ongoing and future research to develop low-cost and effective methods to produce or extract melanin. A plausible solution is biosynthesis of melanin in bacteria.<sup>164</sup> The other barrier is the limited electrical conductivity of melanin. In recent years, some progresses have been made to address this issue. Shim *et al.* achieved electrical conductivities as high as  $1.17 \pm 0.13 \text{ S cm}^{-1}$  by preparing a composite with melanin nanoparticles in a poly(vinyl alcohol) matrix.<sup>165</sup> This was a huge improvement in contrast to the original conductivity of significantly hydrated melanin which was reported to be  $10^{-3} \text{ S cm}^{-1}$ .<sup>166</sup> Meredith *et al.* reported a novel metal (copper(II) ions) doping strategy to enhance and control the proton conductivity of melanin for OECT application.<sup>155</sup> However, there is still much work to do to improve the conductivity of melanin so that it becomes a more competitive OSM for high-performance electronic devices.

### 3.3 Caffeine analogues

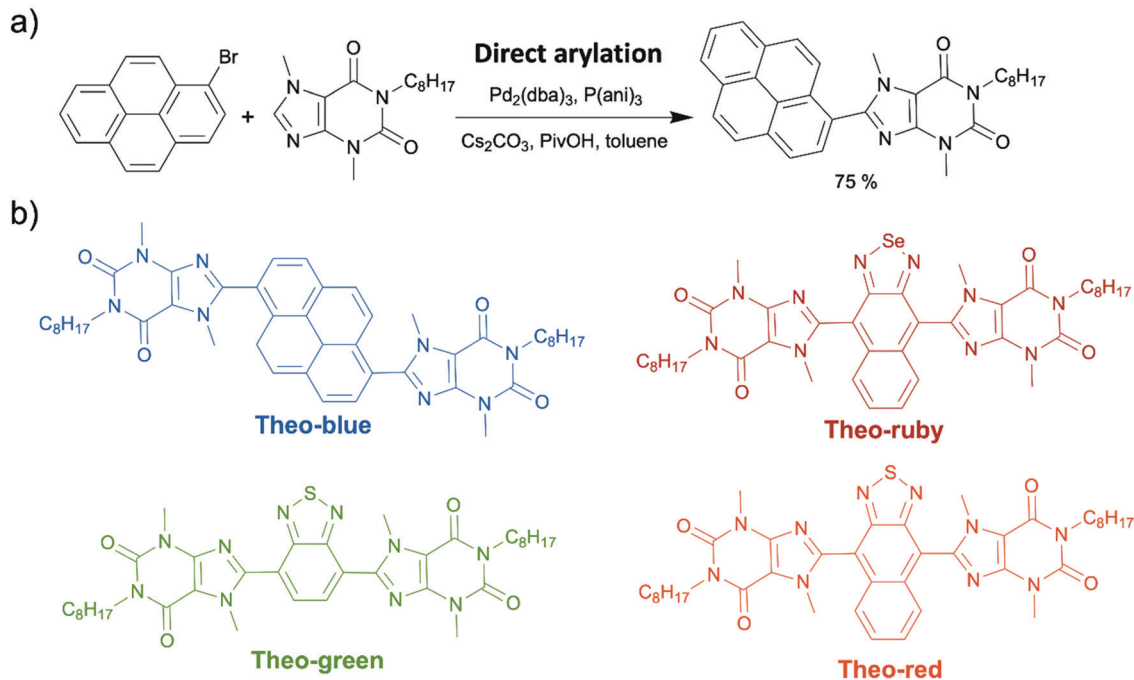
Last but not least, caffeine and some of its analogues, such as theobromine and theophylline, are classified as xanthine alkaloids that were originally discovered in plants, such as cacao plants, tea plants, and coffee beans. They exist in a number of common foods and beverages, including coffee, tea, and chocolate. Currently, these chemicals are industrially produced by decaffeination or biosynthesis from a nucleoside, xanthosine.<sup>167</sup> They are also inexpensive, less than one USD per gram. The xanthine core of caffeine and its analogues contains a five-membered ring, imidazole, fused with a six-membered ring, pyrimidinedione. As the amide functionalities are typically in their zwitterionic resonance forms, the xanthine core is a conjugated planar structure where electrons are delocalized. (Scheme 15).

In sharp contrast to indigo and melanin, the application of caffeine and its naturally occurring analogues in organic



Scheme 15 Xanthine and its zwitterionic resonance structure.





**Scheme 16** (a) Direct arylation to attach alkylated theobromine onto pyrene. (b) The structures of the four synthesized theobromine-based organic dyes (Theo-blue, Theo-green, Theo-ruby, and Theo-red).

electronics has a very short history. In fact, the first OSM synthesized from theobromine was reported by our group in 2019. In that report, we attached alkylated theobromine onto a pyrene luminophore by direct arylation. This worked to suppress aggregation caused quenching (ACQ) in pyrene's solid state (Scheme 16a).<sup>62</sup> The resulted pyrene-theobromine thin films exhibited a photoluminescence quantum yield (PLQY) of almost 100%. After that, we synthesized theobromine-based organic dyes (Theo-green and Theo-red) (Scheme 16b) using alkylated theobromine *via* direct arylation.<sup>168</sup> We demonstrated the stability of Theo-green and Theo-red against photoreduction due to their "acceptor-acceptor" skeleton resulting from electron-withdrawing theobromine and thiadiazole. The organic LED light converter made from theobromine-based organic dyes (1 wt%) and a commercial polymer, poly(styrene-butadiene-styrene) (SBS) (99 wt%), were transparent because of the high solubility of theobromine-based dyes in SBS. The high transparency endowed the organic light converter with high efficiency due to minimal light scattering loss. Additionally, the PLQY of the organic light converter was as high as 90% under ambient conditions. In our other study, we incorporated three organic dyes (Theo-blue, Theo-green, and Theo-ruby) synthesized *via* direct arylation (Scheme 16b) into a light converter in a hybrid LED.<sup>169</sup> Compared to the incumbent inorganic phosphor light converters made from rare-earth elements, the new organic theobromine-based light converter offered improved performance as measured by the color rendering index and color fidelity index, resulting in more continuous and uniform emitted light across visible wavelengths. In addition, owing to the affordability and abundance of the starting material and the excellent atom-economy of the synthetic route, the price of the light converters

could be reduced to 0.013 USD per 1 W LED from approximately 0.192 USD of the commercial products. Overall, our development of novel theobromine-based organic dyes provided a new strategy to produce organic dyes with good structural and spectral tunability using environmentally compatible and abundant natural products.

## 4. Summary and perspective

OSMs have received much attention in the electronics industry due to the advantages they have over the inorganic semiconducting materials. They not only allow for more flexible, stretchable, and lightweight materials, but also are solution processible. More importantly, their properties are tunable by simple modifications to their chemical structures, which enables tailoring properties for a specific application. However, the conventional syntheses of OSMs are not environmentally friendly, which poses severe problems with industrial scale production, where the negative environmental impacts are amplified. In order to improve the environmental friendliness of OSMs, many efforts have been made to minimize chemical waste generation, toxicity of the chemicals used, and energy consumption of the overall synthetic procedures. Despite all the advances made during the past few years as summarized in this review, there is still a long way to go in the pursuit of high-performance and truly environmentally friendly OSMs.

First, oxidative CH/CH coupling has not reached widespread use yet compared to direct arylation and other conventional coupling methods. Future studies should be focused on overcoming the challenges in reactivity and selectivity control, while there is a simultaneous need to expand the substrate scope of



the oxidative CH/CH coupling. Controlled DArPs and oxidative CH/CH polymerizations are desired to achieve consistent semi-conducting polymer products every batch with narrow molecular weight distributions. Secondly, all the chemicals used in the synthesis of OSMs, including solvents, catalysts, and starting materials, need to be non-toxic and innocuous to human health and the environment. Future research should focus on applying earth abundant, bio-based, biocompatible and/or biodegradable substances in OSM syntheses. In addition, the energy consumption of OSM syntheses could be lessened further if the syntheses were able to be conducted under ambient conditions (at room temperature, under atmospheric pressure, and in the air). Finally, the work presented here can provide the foundation and guidance for the future development of eco-friendly, cost-effective, and well-functioning organic electronics.

## Author contributions

All authors contributed to the manuscript. All authors have given approval to the final version of the manuscript.

## Conflicts of interest

There are no conflicts to declare.

## Acknowledgements

This work was supported by the NSF under the CCI Center for Selective CH Functionalization, CHE-1700982. Yunping Huang and Amy L. Mayhugh are gratefully acknowledged for proof-reading the manuscript and for helpful discussions.

## References

- C. Liu, K. Wang, X. Gong and A. J. Heeger, *Chem. Soc. Rev.*, 2016, **45**, 4825.
- S. Holliday, Y. Li and C. K. Luscombe, *Prog. Polym. Sci.*, 2017, **70**, 34.
- M. U. Chaudhry, K. Muhieddine, R. Wawrzinek, J. Li, S.-C. Lo and E. B. Namdas, *ACS Photonics*, 2018, **5**, 2137.
- V. Ahmad, A. Shukla, J. Sobus, A. Sharma, D. Gedefaw, G. G. Andersson, M. R. Andersson, S.-C. Lo and E. B. Namdas, *Adv. Opt. Mater.*, 2018, **6**, 1800768.
- B. G. A. L. Borges, M. Gioti, R. S. Correa, A. K. Andreopoulou, A. G. Veiga, A. Laskarakis, J. K. Kallitsis, S. Logothetidis and M. L. M. Rocco, *Opt. Mater.*, 2021, **117**, 111145.
- H. Sirringhaus, *Adv. Mater.*, 2014, **26**, 1319.
- S. Riera-Galindo, F. Leonardi, R. Pfattner and M. Mas-Torrent, *Adv. Mater. Technol.*, 2019, **4**, 1900104.
- H. Chen, M. Hurhangee, M. Nikolka, W. Zhang, M. Kirkus, M. Neophytou, S. J. Cryer, D. Harkin, P. Hayoz, M. Abdi-Jalebi, C. R. McNeill, H. Sirringhaus and I. McCulloch, *Adv. Mater.*, 2017, **29**, 1702523.
- J. Yang, Z. Zhao, S. Wang, Y. Guo and Y. Liu, *Chem*, 2018, **4**, 2748.
- S. Nambiar and J. T. W. Yeow, *Biosens. Bioelectron.*, 2011, **26**, 1825.
- D. C. Martin, *MRS Commun.*, 2015, **5**, 131.
- A. B. Tamayo, M. Tantiwivat, B. Walker and T.-Q. Nguyen, *J. Phys. Chem. C*, 2008, **112**, 15543.
- X. Shi, A. Sui, Y. Wang, Y. Li, Y. Geng and F. Wang, *Chem. Commun.*, 2015, **51**, 2138.
- J. Kettle, M. Horie, L. A. Majewski, B. R. Saunders, S. Tuladhar, J. Nelson and M. L. Turner, *Sol. Energy Mater. Sol. Cells*, 2011, **95**, 2186.
- C. Kanimozhi, P. Balraju, G. D. Sharma and S. Patil, *J. Phys. Chem. B*, 2010, **114**, 3095.
- B. S. Ong, Y. Wu, Y. Li, P. Liu and H. Pan, *Chem. – Eur. J.*, 2008, **14**, 4766.
- V. Mal'yskiy, J.-J. Simon, L. Patrone and J.-M. Raimundo, *RSC Adv.*, 2015, **5**, 354.
- L. Hrostea, M. Girtan, R. Mallet and L. Leontie, *IOP Conf. Ser.: Mater. Sci. Eng.*, 2018, **374**, 012015.
- T. Fukuda, A. Toda, K. Takahira, K. Suzuki, Y. Liao, M. Hirahara, M. Saito and I. Osaka, *Thin Solid Films*, 2016, **612**, 373.
- J. Swanston, *Ullmann's Encycl. Ind. Chem.*, 2006, **36**, 657.
- Thiophene. Safety Data Sheet number T31801 [online]. Sigma-Aldrich: St. Louis, MO, April 13, 2020. <https://www.sigmaaldrich.com/US/en/sds/aldrich/t31801> (accessed August 14, 2021).
- C. K. Jaladanki, N. Taxak, R. A. Varikoti and P. V. Bharatam, *Chem. Res. Toxicol.*, 2015, **28**, 2364.
- N. Le Dang, T. B. Hughes, G. P. Miller and S. J. Swamidass, *Chem. Res. Toxicol.*, 2017, **30**, 1046.
- A. L. Harreus, *Ullmann's Encycl. Ind. Chem.*, 2000, **30**, 615.
- H. E. Hoydonckx, W. M. Van Rhijn, W. Van Rhijn, D. E. De Vos and P. A. Jacobs, *Ullmann's Encycl. Ind. Chem.*, 2007, **16**, 285.
- T. P. Osedach, T. L. Andrewb and V. Bulović, *Energy Environ. Sci.*, 2013, **6**, 711.
- R. Po, A. Bernardi, A. Calabrese, C. Carbonera, G. Corso and A. Pellegrino, *Energy Environ. Sci.*, 2014, **7**, 925.
- A. Marrocchi, A. Facchetti, D. Lanari, C. Petruccia and L. Vaccaro, *Energy Environ. Sci.*, 2016, **9**, 763.
- I. A. Stepek and K. Itami, *ACS Mater. Lett.*, 2020, **2**, 951.
- J. Kuwabara and T. Kanbara, *Macromol. Rapid Commun.*, 2021, **42**, 2000493.
- Y. Huang and C. K. Luscombe, *Chem. Rec.*, 2019, **19**, 1039.
- J. Kuwabara and T. Kanbara, *Bull. Chem. Soc. Jpn.*, 2019, **92**, 152.
- M. Mooney, A. Nyayachavadi and S. Rondeau-Gagné, *J. Mater. Chem. C*, 2020, **8**, 14645.
- R. M. Pankow and B. C. Thompson, *Polym. Chem.*, 2020, **11**, 630.
- K. Nakabayashi, *Polym. J.*, 2018, **50**, 475.
- J. Kuwabara, *Polym. J.*, 2018, **50**, 1099.
- M. Leclerc, S. Brassard and S. Beaupré, *Polym. J.*, 2020, **52**, 13.
- M. Wakioka and F. Ozawa, *Asian J. Org. Chem.*, 2018, **7**, 1206.





- 39 M. Mainville and M. Leclerc, *ACS Appl. Polym. Mater.*, 2021, **3**, 2.
- 40 N. S. Gobalasingham and B. C. Thompson, *Prog. Polym. Sci.*, 2018, **83**, 135.
- 41 J. Zhang, L. J. Kang, T. C. Parker, S. B. Blakey, C. K. Luscombe and S. R. Marder, *Molecules*, 2018, **23**, 922.
- 42 S. Phan and C. K. Luscombe, *Trends Chem.*, 2019, **1**, 670.
- 43 Y. Huang, D. L. Elder, A. L. Kwiram, S. A. Jenekhe, A. K. Y. Jen, L. R. Dalton and C. K. Luscombe, *Adv. Mater.*, 2021, **33**, 1904239.
- 44 B. M. Trost, *Science*, 1991, **254**, 1471.
- 45 D. Lapointe and K. Fagnou, *Chem. Lett.*, 2010, **39**, 1118.
- 46 K. H. Hendriks, W. Li, G. H. L. Heintges, G. W. P. van Pruissen, M. M. Wienk and R. A. J. Janssen, *J. Am. Chem. Soc.*, 2014, **136**, 11128.
- 47 T. Vangerven, P. Verstappen, J. Drijkoningen, W. Dierckx, S. Himmelberger, A. Salleo, D. Vanderzande, W. Maes and J. V. Manca, *Chem. Mater.*, 2015, **27**, 3726.
- 48 Q. Shi, W. Tatum, J. Zhang, C. Scott, C. K. Luscombe, S. R. Marder and S. B. Blakey, *Asian J. Org. Chem.*, 2018, **7**, 1419.
- 49 M. Wakioka, N. Yamashita, H. Mori, Y. Nishihara and F. Ozawa, *Molecules*, 2018, **23**, 981.
- 50 M. Wakioka, H. Morita, N. Ichihara, M. Saito, I. Osaka and F. Ozawa, *Macromolecules*, 2020, **53**, 158.
- 51 J. Zhang, W. Chen, A. J. Rojas, E. V. Jucov, T. V. Timofeeva, T. C. Parker, S. Barlow and S. R. Marder, *J. Am. Chem. Soc.*, 2013, **135**, 16376.
- 52 J. L. Bon, D. Feng, S. R. Marder and S. B. Blakey, *J. Org. Chem.*, 2014, **79**, 7766.
- 53 Q. Shi, S. Zhang, J. Zhang, V. F. Oswald, A. Amassian, S. R. Marder and S. B. Blakey, *J. Am. Chem. Soc.*, 2016, **138**, 3946.
- 54 Ö. Usluer, M. Abbas, G. Wantz, L. Vignau, L. Hirsch, E. Grana, C. Brochon, E. Cloutet and G. Hadziioannou, *ACS Macro Lett.*, 2014, **3**, 1134.
- 55 R. M. Pankow, L. Ye and B. C. Thompson, *Macromolecules*, 2020, **53**, 3315.
- 56 N. S. Gobalasingham, S. Noh and B. C. Thompson, *Polym. Chem.*, 2016, **7**, 1623.
- 57 J. A. Lee and C. K. Luscombe, *ACS Macro Lett.*, 2018, **7**, 767.
- 58 C. Chen, D. H. Maldonado, D. Le Borgne, F. Alary, B. Lonetti, B. Heinrich, B. Donnioe and K. I. M. Ching, *New J. Chem.*, 2016, **40**, 7326.
- 59 S. M. McAfee and G. C. Welch, *Chem. Rec.*, 2019, **19**, 989.
- 60 S. M. McAfee, A.-J. Payne, S. V. Dayneko, G. P. Kini, C. E. Song, J.-C. Lee and G. C. Welch, *J. Mater. Chem. A*, 2017, **5**, 16907.
- 61 S. M. McAfee, S. V. Dayneko, P. Josse, P. Blanchard, C. Cabanetos and G. C. Welch, *Chem. Mater.*, 2017, **29**, 1309.
- 62 Y. Huang, Y. Liu, P. J. W. Somerville, W. Kaminsky, D. S. Ginger and C. K. Luscombe, *Green Chem.*, 2019, **21**, 6600.
- 63 D. R. Stuart and K. Fagnou, *Science*, 2007, **316**, 1172.
- 64 J.-R. Liu, Y.-Q. Duan, S.-Q. Zhang, L.-J. Zhu, Y.-Y. Jiang, S. Bi and X. Hong, *Org. Lett.*, 2019, **21**, 2360.
- 65 L. J. Kang, L. Xing and C. K. Luscombe, *Polym. Chem.*, 2019, **10**, 486.
- 66 H. Aoki, H. Saito, Y. Shimoyama, J. Kuwabara, T. Yasuda and T. Kanbara, *ACS Macro Lett.*, 2018, **7**, 90.
- 67 Q. Zhang, M. Chang, Y. Lu, Y. Sun, C. Li, X. Yang, M. Zhang and Y. Chen, *Macromolecules*, 2018, **51**, 379.
- 68 Y. Shimoyama, J. Kuwabara and T. Kanbara, *ACS Catal.*, 2020, **10**, 3390.
- 69 J. Li, D. Han, Q. Zhang, Z. He and Y. Lu, *J. Polym. Sci.*, 2021, **59**, 240.
- 70 X. C. Cambeiro, N. Ahlsten and I. Larrosa, *J. Am. Chem. Soc.*, 2015, **137**, 15636.
- 71 H. Saito, J. Kuwabara, T. Yasuda and T. Kanbara, *Polym. Chem.*, 2016, **7**, 2775.
- 72 H. Saito, J. Kuwabara, T. Yasuda and T. Kanbara, *Macromol. Rapid Commun.*, 2018, **39**, 1800414.
- 73 R. Iwamori, R. Sato, J. Kuwabara, T. Yasuda and T. Kanbara, *Macromol. Rapid Commun.*, 2021, 2100283.
- 74 S. Murai, *Activation of Unreactive Bonds and Organic Synthesis*, Springer, New York, 1999.
- 75 P. P. Khlyabich, B. Burkhart, A. E. Rudenko and B. C. Thompson, *Polymer*, 2013, **54**, 5267.
- 76 A. L. Mayhugh and C. K. Luscombe, *Beilstein J. Org. Chem.*, 2020, **16**, 384.
- 77 L. Boisvert and K. I. Goldberg, *Acc. Chem. Res.*, 2012, **45**, 899.
- 78 M. L. Scheuermann and K. I. Goldberg, *Chem. – Eur. J.*, 2014, **20**, 14556.
- 79 A. Ichige, H. Saito, J. Kuwabara, T. Yasuda, J.-C. Choi and T. Kanbara, *Macromolecules*, 2018, **51**, 6782.
- 80 X. Chen, A. Ichige, J. Chen, I. Fukushima, J. Kuwabara and T. Kanbara, *Polymer*, 2020, **207**, 122927.
- 81 A. Faradhiyani, Q. Zhang, K. Maruyama, J. Kuwabara, T. Yasudab and T. Kanbara, *Mater. Chem. Front.*, 2018, **2**, 1306.
- 82 D. J. C. Constable, P. J. Dunn, J. D. Hayler, G. R. Humphrey, J. L. Leazer, Jr., R. J. Linderman, K. Lorenz, J. Manley, B. A. Pearlman, A. Wells, A. Zaksh and T. Y. Zhang, *Green Chem.*, 2007, **9**, 411.
- 83 P. T. Anastas and M. M. Kirchhoff, *Acc. Chem. Res.*, 2002, **35**, 686.
- 84 D. Prat, J. Hayler and A. Wells, *Green Chem.*, 2014, **16**, 4546.
- 85 D. F. Aycock, *Org. Process Res. Dev.*, 2007, **11**, 156.
- 86 J. J. Dong, J. Roger, C. Verrier, T. Martin, R. Le Goff, C. Hoarau and H. Doucet, *Green Chem.*, 2010, **12**, 2053.
- 87 K. Beydoun and H. Doucet, *ChemSusChem*, 2011, **4**, 526.
- 88 G. Strappaveccia, E. Ismalaj, C. Petrucci, D. Lanari, A. Marrocchi, M. Drees, A. Facchetti and L. Vaccaro, *Green Chem.*, 2015, **17**, 365.
- 89 J. Sherwood, J. H. Clark, I. J. S. Fairlamb and J. M. Slattery, *Green Chem.*, 2019, **21**, 2164.
- 90 R. M. Pankow, L. Ye, N. S. Gobalasingham, N. Salami, S. Samal and B. C. Thompson, *Polym. Chem.*, 2018, **9**, 3885.
- 91 D. Conelli, N. Margiotta, R. Grisorio and G. P. Suranna, *Macromol. Chem. Phys.*, 2021, **222**, 2000382.
- 92 C. M. Alder, J. D. Hayler, R. K. Henderson, A. M. Redman, L. Shukla, L. E. Shuster and H. F. Sneddon, *Green Chem.*, 2016, **18**, 3879.
- 93 R. M. Pankow, L. Ye and B. C. Thompson, *Polym. Chem.*, 2019, **10**, 4561.



- 94 L. Ye, R. M. Pankow, M. Horikawa, E. L. Melenbrink, K. Liu and B. C. Thompson, *Macromolecules*, 2019, **52**, 9383.
- 95 T. M. Pappenfus, F. Almyahi, N. A. Cooling, E. W. Culver, S. C. Rasmussen and P. C. Dastoor, *Macromol. Chem. Phys.*, 2018, **219**, 1800272.
- 96 L. Ye and B. C. Thompson, *ACS Macro Lett.*, 2021, **10**, 714.
- 97 J. H. Clark, D. J. Macquarrie and J. Sherwood, *Green Chem.*, 2012, **14**, 90.
- 98 F. Grenier, K. Goudreau and M. Leclerc, *J. Am. Chem. Soc.*, 2017, **139**, 2816.
- 99 H. Ayalew, T.-L. Wang, T.-H. Wang, H.-F. Hsu and H.-H. Yu, *Synlett*, 2018, 2660.
- 100 Y.-J. Lin, H.-S. Sun, H.-R. Yang, Y.-Y. Lai, K.-Y. Hou and Y.-H. Liu, *Macromol. Rapid Commun.*, 2020, **41**, 2000021.
- 101 R. J. Lundgren and M. Stradiotto, *Chem. – Eur. J.*, 2012, **18**, 9758.
- 102 H. Li, C. C. C. Johansson Seechurn and T. J. Colacot, *ACS Catal.*, 2012, **2**, 1147.
- 103 A. Kumbhar, *J. Organomet. Chem.*, 2017, **848**, 22.
- 104 L. Giraud, S. Grelier, E. Grau, G. Hadziioannou, C. Brochon, H. Cramail and E. Cloutet, *J. Mater. Chem. C*, 2020, **8**, 9792.
- 105 J. Huang, J. Chan, Y. Chen, C. J. Borths, K. D. Baucom, R. D. Larsen and M. M. Faul, *J. Am. Chem. Soc.*, 2010, **132**, 3674.
- 106 Q. Huang, X. Qin, B. Li, J. Lan, Q. Guo and J. You, *Chem. Commun.*, 2014, **50**, 13739.
- 107 R. M. Pankow, L. Ye and B. C. Thompson, *Polym. Chem.*, 2018, **9**, 4120.
- 108 R. M. Pankow, L. Ye and B. C. Thompson, *ACS Macro Lett.*, 2018, **7**, 1232.
- 109 L. Ye, R. M. Pankow, A. Schmitt and B. C. Thompson, *Polym. Chem.*, 2019, **10**, 6545.
- 110 L. Ye, A. Schmitt, R. M. Pankow and B. C. Thompson, *ACS Macro Lett.*, 2020, **9**, 1446.
- 111 E. B. Merkushev, *Synthesis*, 1988, 923.
- 112 H. I. Patil, M. C. Singh, P. Gaikwad, K. S. Lade, N. A. Gadhave and S. D. Sawant, *J. Pharm. Res.*, 2011, **4**, 4798.
- 113 V. R. Feig, H. Tran and Z. Bao, *ACS Cent. Sci.*, 2018, **4**, 337.
- 114 Y. Cao and K. E. Uhrich, *J. Bioact. Compat. Polym.*, 2019, **34**, 3.
- 115 E. D. Głowacki, G. Voss, L. Leonat, M. Irimia-Vladu, S. Bauer and N. S. Sariciftci, *Isr. J. Chem.*, 2012, **52**, 540.
- 116 Y. Hiroyuki, Organic transistor, JP 098454A, 2008.
- 117 M. Irimia-Vladu, E. D. Głowacki, P. A. Troshin, G. Schwabegger, L. Leonat, D. K. Susarova, O. Krystal, M. Ullah, Y. Kanbur, M. A. Bodea, V. F. Razumov, H. Sitter, S. Bauer and N. S. Sariciftci, *Adv. Mater.*, 2012, **24**, 375.
- 118 M. Irimia-Vladu, Y. Kanbur, F. Camaioni, M. E. Coppola, C. Yumusak, C. V. Irimia, A. Vlad, A. Operamolla, G. M. Farinola, G. P. Suranna, N. Gonzalez-Benitez, M. C. Molina, L. F. Bautista, H. Langhals, B. Stadlober, E. D. Głowacki and N. S. Sariciftci, *Chem. Mater.*, 2019, **31**, 6315.
- 119 D. V. Anokhin, L. I. Leshanskaya, A. A. Piryazev, D. K. Susarova, N. N. Dremova, E. V. Shcheglov, D. A. Ivanov, V. F. Razumov and P. A. Troshin, *Chem. Commun.*, 2014, **50**, 7639.
- 120 M. A. Manthrammel, I. S. Yahia, M. Shkir, S. AlFaify, H. Y. Zahran, V. Ganesh and F. Yakuphanoglu, *Solid State Sci.*, 2019, **93**, 7.
- 121 A. Rivalta, C. Albonetti, D. Biancone, M. D. Ciana, S. d'Agostino, L. Biniek, M. Brinkmann, A. Giunchi, T. Salzillo, A. Brillante, R. G. D. Valle and E. Venuti, *Surf. Interfaces*, 2021, **24**, 101058.
- 122 E. D. Głowacki, G. Voss, K. Demirak, M. Havlicek, N. Sünger, A. C. Okur, U. Monkowius, J. Gąsiorowski, L. Leonat and N. S. Sariciftci, *Chem. Commun.*, 2013, **49**, 6063.
- 123 C. Guo, B. Sun, J. Quinn, Z. Yan and Y. Li, *J. Mater. Chem. C*, 2014, **2**, 4289.
- 124 C. Guo, J. Quinn, B. Sun and Y. Li, *J. Mater. Chem. C*, 2015, **3**, 5226.
- 125 C. Liu, S. Dong, P. Cai, P. Liu, S. Liu, J. Chen, F. Liu, L. Ying, T. P. Russell, F. Huang and Y. Cao, *ACS Appl. Mater. Interfaces*, 2015, **7**, 9038.
- 126 J. H. L. Ngai, G. Y. Chang, X. Gao, X. Zhou, A. D. Hendsbee and Y. Li, *RSC Adv.*, 2019, **9**, 26230.
- 127 E. D. Głowacki, G. Voss and N. S. Sariciftci, *Adv. Mater.*, 2013, **25**, 6783.
- 128 I. V. Klimovich, L. I. Leshanskaya, S. I. Troyanov, D. V. Anokhin, D. V. Novikov, A. A. Piryazev, D. A. Ivanov, N. N. Dremova and P. A. Troshin, *J. Mater. Chem. C*, 2014, **2**, 7621.
- 129 S.-F. Zhang, X.-K. Chen, J.-X. Fan and A.-M. Ren, *Org. Electron.*, 2015, **24**, 12.
- 130 O. Pitayatanakul, T. Higashino, T. Kadoya, M. Tanaka, H. Kojima, M. Ashizawa, T. Kawamoto, H. Matsumoto, K. Ishikawa and T. Mori, *J. Mater. Chem. C*, 2014, **2**, 9311.
- 131 M. Irimia-Vladu, E. D. Głowacki, G. Voss, S. Bauer and N. S. Sariciftci, *Mater. Today*, 2012, **15**, 340.
- 132 K.-Y. Choi, *Dyes Pigm.*, 2020, **181**, 108570.
- 133 G. Engi, *Angew. Chem.*, 1914, **27**, 144.
- 134 B. He, A. B. Pun, D. Zherebetsky, Y. Liu, F. Liu, L. M. Klivansky, A. M. McGough, B. A. Zhang, K. Lo, T. P. Russell, L. Wang and Y. Liu, *J. Am. Chem. Soc.*, 2014, **136**, 15093.
- 135 M. A. Kolaczowski and Y. Liu, *Chem. Rec.*, 2019, **19**, 1062.
- 136 K. J. Fallon and H. Bronstein, *Acc. Chem. Res.*, 2021, **54**, 182.
- 137 G. Summers and E. Gibson, *ChemPhotoChem*, 2018, **2**, 498.
- 138 A. Shukla, N. R. Wallwork, X. Li, J. Sobus, V. T. N. Mai, S. K. M. McGregor, K. Chen, R. J. Lepage, E. H. Krenske, E. G. Moore, E. B. Namdas and S.-C. Lo, *Adv. Opt. Mater.*, 2020, **8**, 1901350.
- 139 F. Solano, *New J. Sci.*, 2014, **2014**, 1.
- 140 V. P. Grishchuk, S. A. Davidenko, I. D. Zholner, A. B. Verbitskii, M. V. Kurik and Y. P. Piryatinskii, *Tech. Phys. Lett.*, 2002, **28**, 896.
- 141 P. Meredith and T. Sarna, *Pigm. Cell Res.*, 2006, **19**, 572.
- 142 E. Vahidzadeh, A. P. Kalra and K. Shankar, *Biosens. Bioelectron.*, 2018, **122**, 127.
- 143 T. Ligonzo, M. Ambrico, V. Augelli, G. Perna, L. Schiavulli, M. A. Tamma, P. F. Biagi, A. Minafra and V. Capozzi, *J. Non-Cryst. Solids*, 2009, **355**, 1221.
- 144 P. R. Crippa, V. Cristofolletti and N. Romeo, *Biochim. Biophys. Acta, Gen. Subj.*, 1978, **538**, 164.



- 145 R. Micillo, L. Panzella, M. Iacomino, G. Prampolini, I. Cacelli, A. Ferretti, O. Crescenzi, K. Koike, A. Napolitano and M. d'Ischia, *Sci. Rep.*, 2017, **7**, 41532.
- 146 J. McGinness, P. Corry and P. Proctor, *Science*, 1974, **183**, 853.
- 147 M. R. Powell and B. Rosenberg, *J. Bioenerg.*, 1970, **1**, 493.
- 148 A. B. Mostert, B. J. Powell, I. R. Gentle and P. Meredith, *Appl. Phys. Lett.*, 2012, **100**, 093701.
- 149 A. B. Mostert, B. J. Powell, F. L. Pratt, G. R. Hanson, T. Sarna, I. R. Gentle and P. Meredith, *Proc. Natl. Acad. Sci. U. S. A.*, 2012, **109**, 8943.
- 150 G. Mula, L. Manca, S. Setzu and A. Pezzella, *Nanoscale Res. Lett.*, 2012, **7**, 377.
- 151 A. Antidormi, C. Melis, E. Canadell and L. Colombo, *J. Phys. Chem. C*, 2017, **121**, 11576.
- 152 L. Migliaccio, S. Aprano, L. Iannuzzi, M. G. Maglione, P. Tassini, C. Minarini, P. Manini and A. Pezzella, *Adv. Electron. Mater.*, 2017, **3**, 1600342.
- 153 N. Gogurla, B. Roy, K. Min, J.-Y. Park and S. Kim, *Adv. Mater. Technol.*, 2020, **5**, 1900936.
- 154 M. Sheliakina, A. B. Mostert and P. Meredith, *Mater. Horiz.*, 2018, **5**, 256.
- 155 A. B. Mostert, S. B. Rienecker, M. Sheliakina, P. Zierrep, G. R. Hanson, J. R. Harmer, G. Schenk and P. Meredith, *J. Mater. Chem. B*, 2020, **8**, 8050.
- 156 T.-F. Wu and J.-D. Hong, *Sens. Actuators, B*, 2016, **224**, 178.
- 157 T.-F. Wu, B.-H. Wee and J.-D. Hong, *Adv. Mater. Interfaces*, 2015, **2**, 1500203.
- 158 M. P. da Silva, J. C. Fernandes, N. B. de Figueiredo, M. Congiu, M. Mulato and C. F. de Oliveira Graeff, *AIP Adv.*, 2014, **4**, 037120.
- 159 C. J. Bettinger, J. P. Bruggeman, A. Misra, J. T. Borenstein and R. Langer, *Biomaterials*, 2009, **30**, 3050.
- 160 M. Piacenti-Silva, A. A. Matos, J. V. Paulin, R. A. d. S. Alavarce, R. C. de Oliveira and C. F. Graeff, *Polym. Int.*, 2016, **65**, 1347.
- 161 Y. J. Kim, W. Wu, S.-E. Chun, J. F. Whitacre and C. J. Bettinger, *Proc. Natl. Acad. Sci. U. S. A.*, 2013, **110**, 20912.
- 162 Y. J. Kim, W. Wu, S.-E. Chun, J. F. Whitacre and C. J. Bettinger, *Adv. Mater.*, 2014, **26**, 6572.
- 163 H. Coskun, A. Aljabour, T. Greunz, M. Kehrler, D. Stifter and P. Stadler, *Adv. Sustainable Syst.*, 2021, **5**, 2000176.
- 164 M. E. Pavan, N. I. López and M. J. Pettinari, *Appl. Microbiol. Biotechnol.*, 2020, **104**, 1357.
- 165 T. Eom, J. Jeon, S. Lee, K. Woo, J. E. Heo, D. C. Martin, J. J. Wie and B. S. Shim, *Part. Part. Syst. Charact.*, 2019, **36**, 1900166.
- 166 J. Wünsche, Y. X. Deng, P. Kumar, E. Di Mauro, E. Josberger, J. Sayago, A. Pezzella, F. Soavi, F. Cicoira, M. Rolandi and C. Santato, *Chem. Mater.*, 2015, **27**, 436.
- 167 H. Ashihara, T. Yokota and A. Crozier, *Adv. Bot. Res.*, 2013, **68**, 111.
- 168 Y. Huang, T. A. Cohen, P. J. W. Sommerville and C. K. Luscombe, *J. Mater. Chem. C*, 2021, **9**, 7274.
- 169 Y. Huang, T. A. Cohen and C. K. Luscombe, *Adv. Sustainable Syst.*, 2021, 2000300.

